



Science and
Technology
Facilities Council

RAL Space

Analysis of the Long-Term Performance of the Sentinel-3 SLSTR Instruments

D.L. Smith, E. Polehampton, M. Etxaluze

7th December 2021

This work was funded by the EU
under the Copernicus Program



Contents

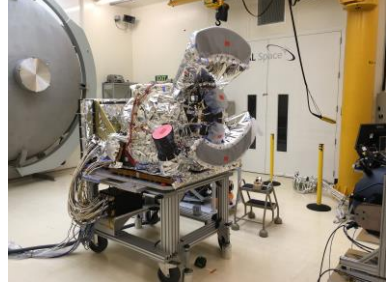
- Introduction
- L0 Monitoring Tools
- Dynamic Range
- FEE Updates
- Thermal Analysis
- Incorporating Uncertainty Analysis in L0 Monitoring
- Updates to MapNoiS3
- Lunar Calibration

Introduction

2016 – Sentinel 3A



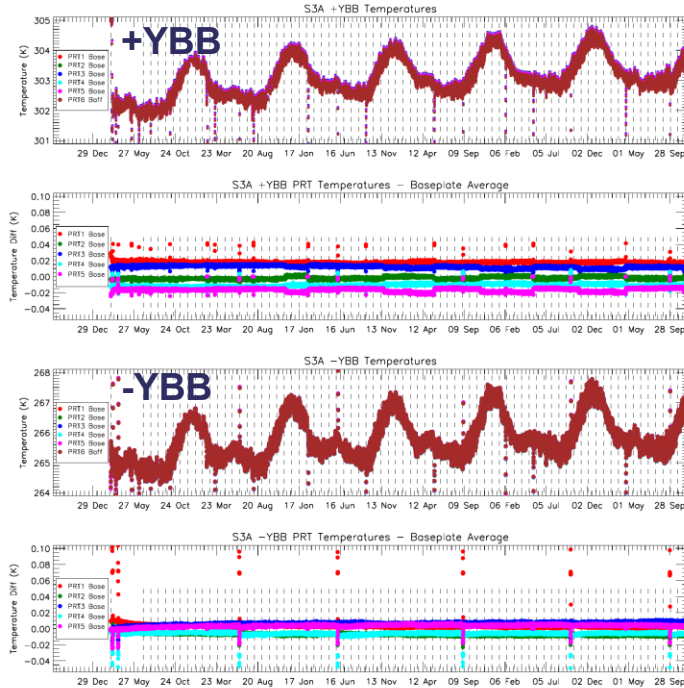
2018 – Sentinel 3B



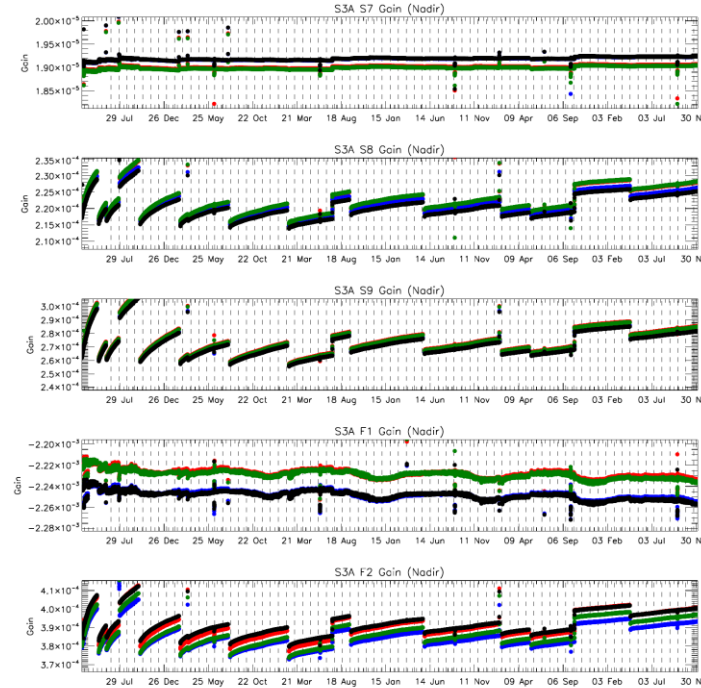
- The Copernicus Sentinel-3 missions are mid-way through their planned operational lifetimes (7.5 years)
 - S3A launched in Feb 2016 – (>5 years)
 - S3B launched in April 2018 – (>3 years)
- SLSTR-C launch not before 2023
 - Full calibration expected Q1 2023
- How are instruments performing and what are expectations longer-term?
- Need for more autonomous monitoring and to maintain performance within operational limits.
- How do we take into account on-orbit performance in L1 uncertainties?

On-Orbit Monitoring

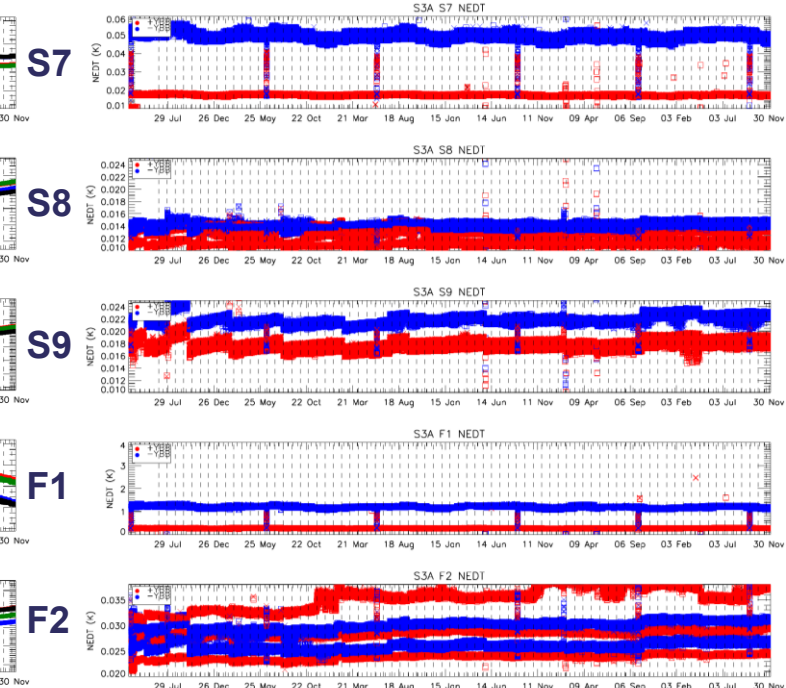
- Routine monitoring of key instrument parameters allows us to
 - Assess low level data quality
 - Demonstrate instrument performance and stability



BB Temperatures



Gain Stability



Radiometric Noise

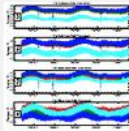
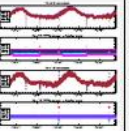
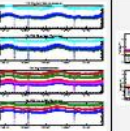
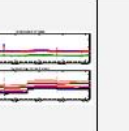
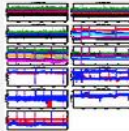
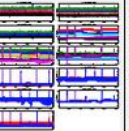
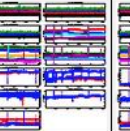
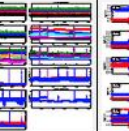
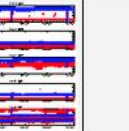
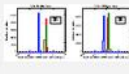
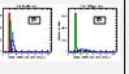
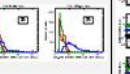
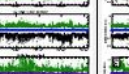
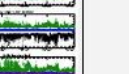
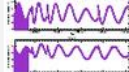
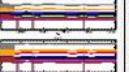
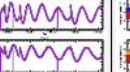
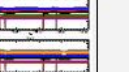
SLSTR L0 Monitoring at RAL

- In order to monitor SLSTR instrument performance, we need to look at raw Level-0 data, for example to,
 - check for gaps in packet stream
 - access all HK parameters (i.e. temperatures, cooler status, etc.)
 - access detector counts for all targets
 - analyse scanner positions/jitter
 - make independent check of L1 calibration parameters
- Raw L0 data are arranged as a stream of binary packets
- RAL tools are written in IDL to decode, sort and plot the data from the packet stream

SLSTR L0 Monitoring at RAL

The RAL monitoring system consists of:

- Level-0 reader and housekeeping data conversion
- Extraction and processing tools
- Control script to process individual orbits
 - Plot functions for each parameter over a single orbit
 - Output CSV files on ISP timescales
 - VISCAL processing
 - Orbital averages added to long term trend files
- Control script to process long term trends
 - Cycle-by-cycle trend plots
 - Yearly trend plots
 - Overall mission plots
 - Cycle-by-cycle parameter summary
- Web pages to display plots and output parameters

S3A Long-term Trends						
	Baff temp	BB temp	OME temp	Detector temp		
Temperatures						
	Noise (Nadir BB1)	Noise (Nadir BB2)	Noise (Obl BB1)	Noise (Obl BB2)	NEDT	
Noise						
	Scanner mean jitter histograms	Scanner stddev jitter histograms	Scanner max-min jitter histograms	Scanner Jitter (Nad view)	Scanner Jitter (Obl view)	
Scanner						
	IPF VSX (Nad VIS)	IPF VSX (Nadir SWIR)	IPF VSX (Obl VIS)	IPF VSX (Obl SWIR)		
VISCAL (IPF L1 ADFs)						

SLSTR L0 Monitoring at RAL

- Plots produced of trends within each orbit, each cycle, each year & whole mission
→ gives a reference library of plots to use when investigating issues
- Calibration parameters independently calculated from L0
- Summary files produced with orbital average parameters
- Summary tables of SNR & NEDT for each cycle
- Links to the Cal/Val plan

Key to alerts:

ALERT	WARN	NOISE	INCOMPLETE	NONE
-------	------	-------	------------	------

Date (Cycle_79)	Orbit Number (relative)																L3 (VIS)	L3 (S8 TIR)	L3 (cloud)
04-Dec-2021	187	188	189	190	191	192	193	194	195	196	197	198	199	200					
03-Dec-2021	173	174	175	176	177	178	179	180	181	182	183	184	185	186					
02-Dec-2021	159	160	161	162	163	164	165	166	167	168	169	170	171	172					
01-Dec-2021	144	145	146	147	148	149	150	151	152	153	154	155	156	157	158				
30-Nov-2021	130	131	132	133	134	135	Orbit Number 24												
29-Nov-2021	116	117	118	119	120	121	22-Nov-2021 14:21:27 - 16:02:26												
28-Nov-2021	102	103	104	105	106	107													
27-Nov-2021	87	88	89	90	91	92													
25-Nov-2021	59	60	61	62	63	64													
24-Nov-2021	44	45	46	47	48	49													
23-Nov-2021	30	31	32	33	34	35													
22-Nov-2021	16	17	18	19	20	21													
Description							Plots												
Missing packets							Missing packets detected												
Counts Histogram																			
Swath Average																			
Count Trend																			
Counts Image																			
Black Body Temperatures																			

S3A Long-term Trends						
	Baff temp	BB temp	OME temp	Detector temp		
Temperatures						
Noise	Noise (Nadir BB1)	Noise (Nadir BB2)	Noise (Obl BB1)	Noise (Obl BB2)	NEDT	
Scanner	Scanner mean jitter histograms	Scanner stddev jitter histograms	Scanner max-min jitter histograms	Scanner Jitter (Nad view)	Scanner Jitter (Obl view)	
	IDE VCV	IDE VCV	IDE VCV (Obl)	IDE VCV (Obl)		

Summary of NEDT per cycle for +YBB (hot) averaged over detectors, integrators and views

	CYCLE_6	CYCLE_7	CYCLE_8	CYCLE_9	CYCLE_10	CYCLE_11	CYCLE_12	CYCLE_13	CYCLE_14	CYCLE_15	CYCLE_16	CYCLE_17	CYCLE_18	CYCLE_19	CYCLE_20	CYCLE_21	CYCLE_22	CYCLE_23	CYCLE_24
S7	17.5	17.7	17.5	17.3	17.2	16.9	16.9	16.8	16.9	17.2	17.2	17.2	18.1	17.2	17.2	17.1	17.2	16.9	16.7
S8	11.2	11.7	11.8	11.3	10.9	11.0	11.0	11.1	11.0	10.9	10.9	11.0	11.1	11.0	11.1	10.9	10.9	10.9	10.8
S9	17.5	19.2	19.5	18.1	17.1	17.4	17.7	17.9	17.6	17.0	17.0	17.2	17.5	17.4	17.5	16.7	16.9	17.0	17.0
F1	272.7	274.0	273.7	268.6	264.9	260.1	259.7	260.3	260.3	267.6	268.3	271.0	297.3	276.3	276.4	269.0	269.9	265.3	263.5
F2	27.6	28.5	28.3	27.7	27.5	27.7	28.0	28.0	27.9	27.6	27.6	27.8	27.8	27.8	27.8	27.4	27.6	27.7	27.8

Summary of NEDT per cycle for -YBB (cold) averaged over detectors, integrators and views

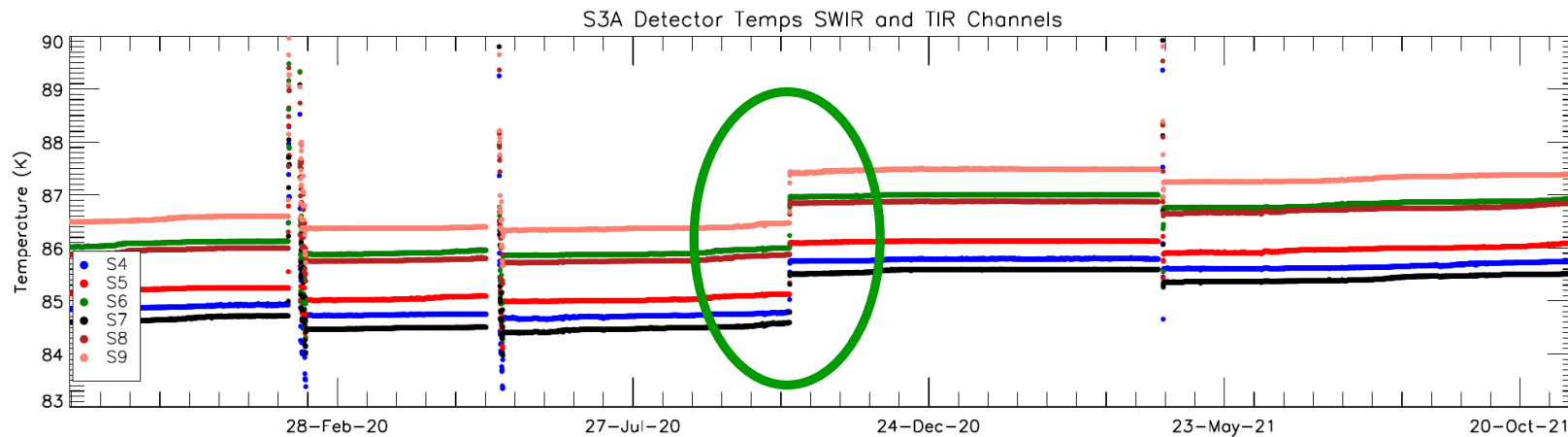
	CYCLE_6	CYCLE_7	CYCLE_8	CYCLE_9	CYCLE_10	CYCLE_11	CYCLE_12	CYCLE_13	CYCLE_14	CYCLE_15	CYCLE_16	CYCLE_17	CYCLE_18	CYCLE_19	CYCLE_20	CYCLE_21	CYCLE_22	CYCLE_23	CYCLE_24
S7	50.7	51.3	51.1	49.3	48.1	47.2	46.6	46.8	47.9	48.7	49.0	48.8	46.9	49.2	49.4	49.4	49.0	47.6	48.2
S8	14.5	15.3	15.3	14.7	14.4	14.4	14.5	14.4	14.4	14.2	14.2	14.3	14.2	14.3	14.4	14.2	14.1	14.2	14.9
S9	22.1	24.4	24.7	22.7	21.5	21.8	22.2	22.4	22.1	21.3	21.4	21.6	21.6	22.0	22.0	21.1	21.3	21.4	21.4
F1	1278.8	1226.2	1229.6	1220.1	1209.0	1162.1	1122.6	1129.8	1177.5	1221.6	1190.9	1198.7	1162.8	1231.2	1233.0	1212.4	1201.6	1161.2	1166.1
F2	29.8	31.5	31.8	30.2	29.3	29.5	29.6	29.6	29.6	29.2	29.3	29.3	29.4	29.6	29.7	29.2	29.2	29.3	29.7

SLSTR L0 Monitoring at EUMETSAT

- In 2019, we completed a short project to update & improve RAL monitoring tools and install at EUMETSAT
 - Has been running internally at EUMETSAT
 - Allows outputs from L0 to be plotted in EUM interactive system
 - Alerts for each parameter (threshold tests)
- In the current project, we have made updates to this monitoring system:
 - Added dynamic range trends for thermal channels S8 and S9
 - Defined method to determine a new commanded detector offset voltage in order to adjust the dynamic range
 - Added uncertainty trends for thermal channels
 - Implement bug fixes and minor improvements
 - Streamline compilation and installation procedure

Dynamic Range

- Response of the IR channels are particularly sensitive to the detector and optics temperatures
- For channel S8 and S9, the response directly affects the dynamic range (limited by digital signal between 0 and 65535 counts)

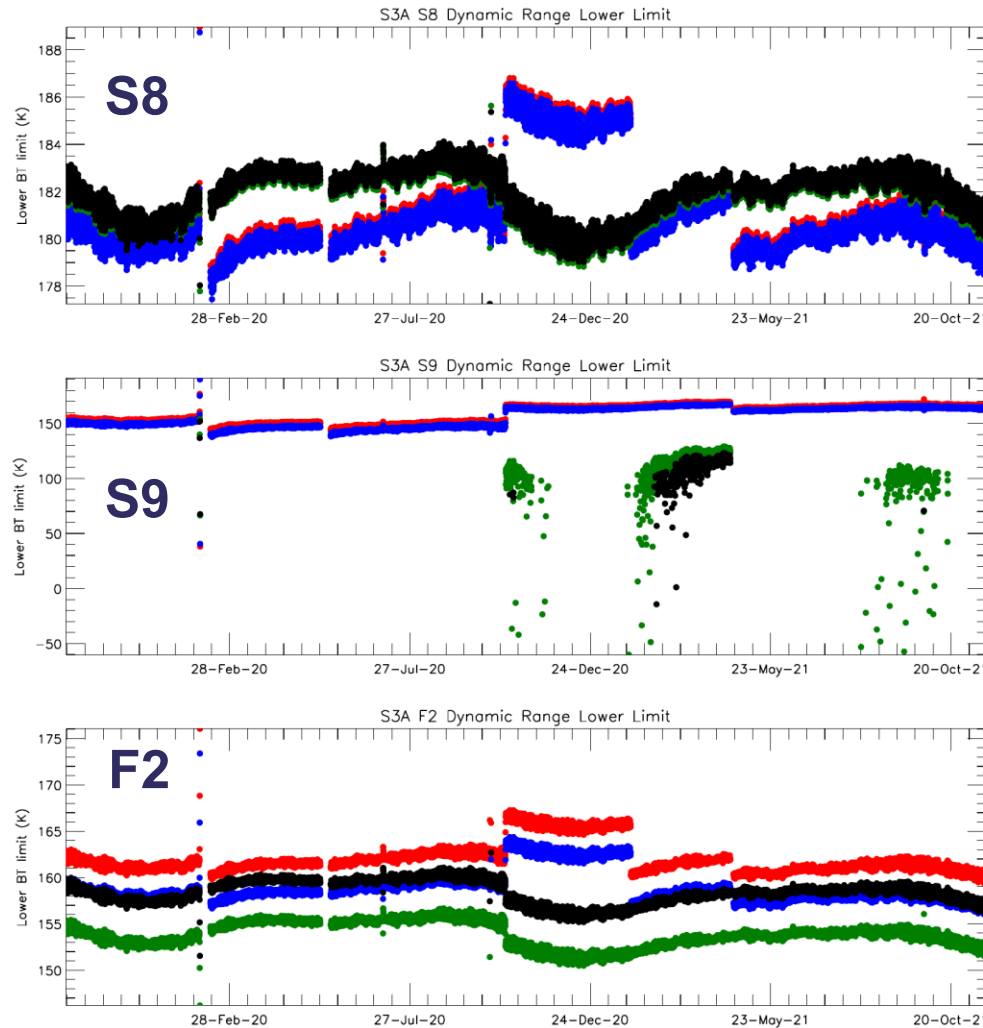


S3A IR channel detector temperature from Oct 2019 to Nov 2021

- Three variations in detector temperature:
 - Orbital cycle, magnitude 0.02 K
 - Gradual rise following decontaminations, magnitude ~0.2K
 - Commanded changes in cooler set-point, magnitude 1-2K
- Cooler cold finger set-point results in step change in temperature, and dynamic range

Dynamic Range Trends

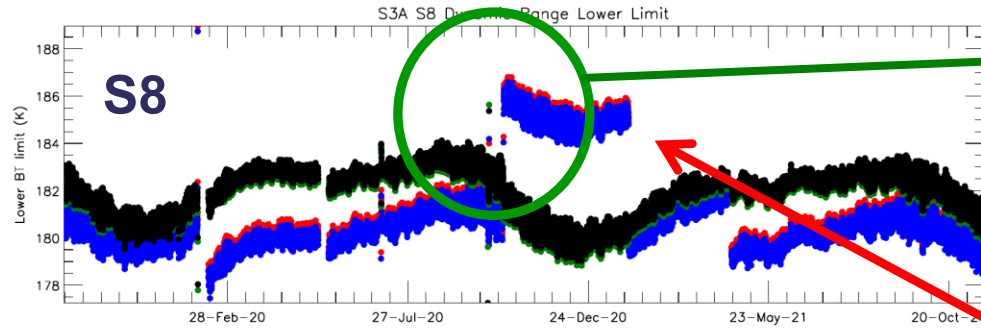
S3A dynamic range lower limit from Oct 2019 to Nov 2021



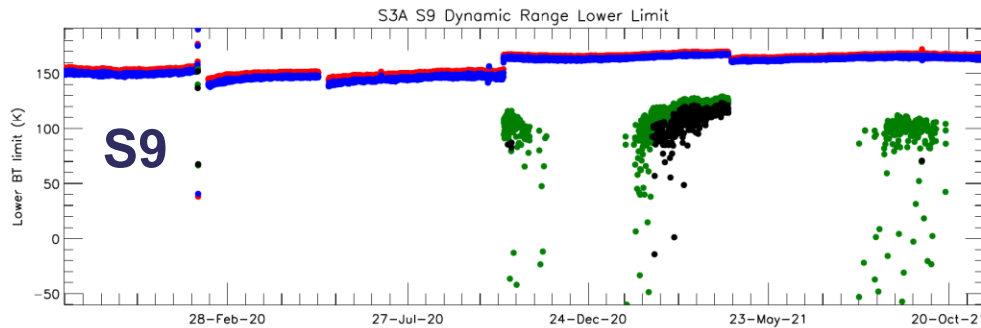
- Dynamic range can be calculated by calibrating 0 and 65535 counts to BT
- Uses the measured radiometric gain/offset
- Each detector and integrator has a slightly different range (shown in different colours)
- Dynamic range also depends on the commanded voltage offset applied to the detectors

Dynamic Range Trends

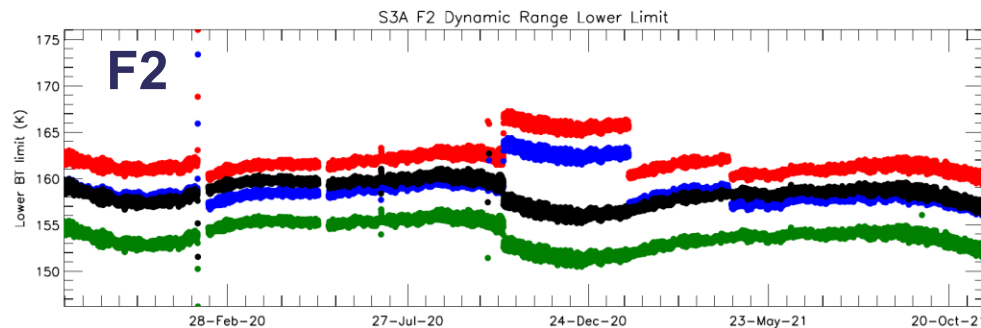
S3A dynamic range lower limit from Oct 2019 to Nov 2021



After cooler set point change, one S8 detector lower limit changed

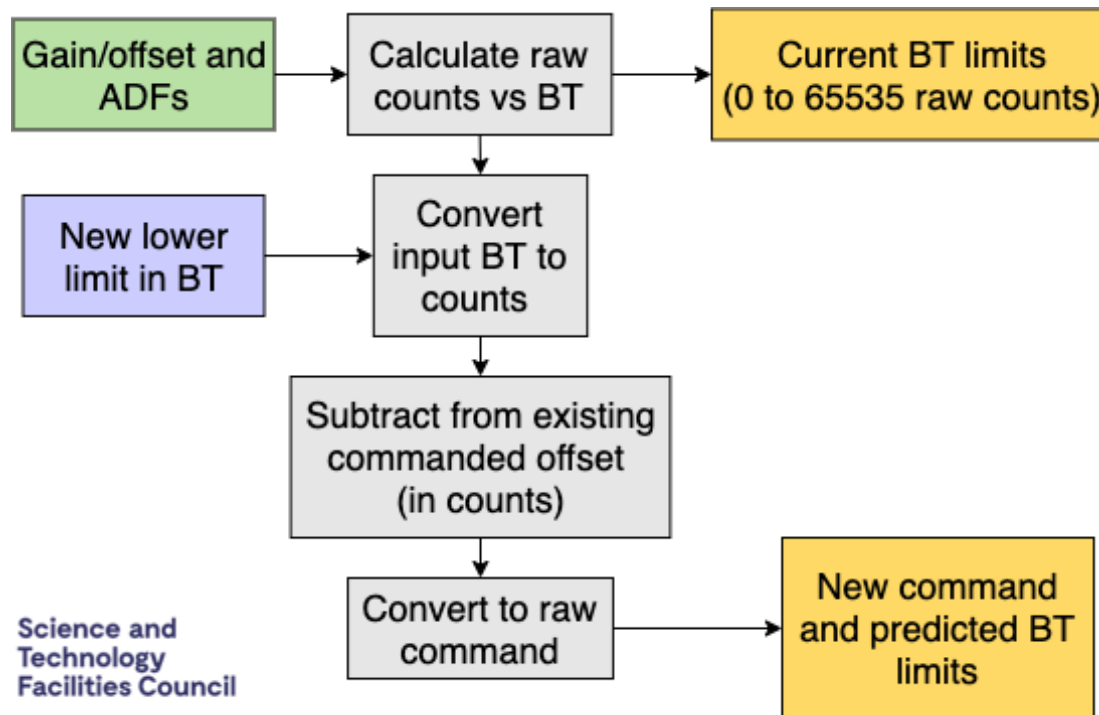


Commanded detector offset voltage can be used to adjust dynamic range



Commanded voltage offset calculator

- After a detector temperature change, the commanded detector voltage offset can be used to re-adjust dynamic range
- Need to calculate the best command corresponding to desired range
- We have defined a procedure to calculate the best commanded offset and predict its effect



This procedure has been used to re-adjust the dynamic range after previous SLSTR cooler cold tip temperature changes

Thermal Analysis

- L0 monitoring provides time series of instrument temperatures for key sub-systems.

Blackbodies, Optics, Mechanisms

- We want to use the data to evaluate the trends and estimate future performance.
- For no-cryogenic temperatures, the long-term temperature trends comprise 2 main components

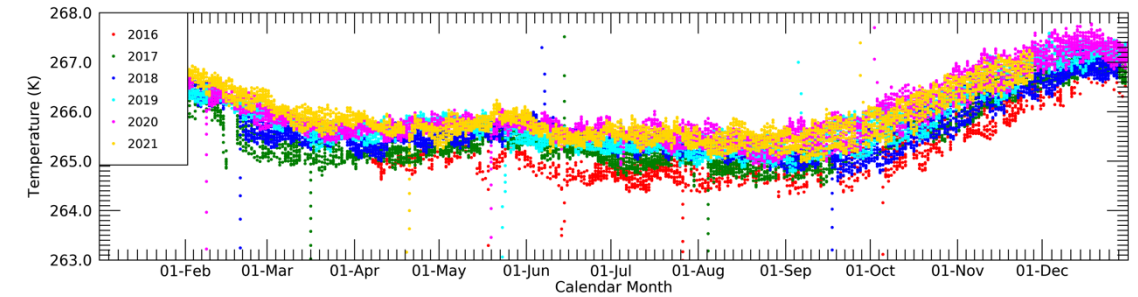
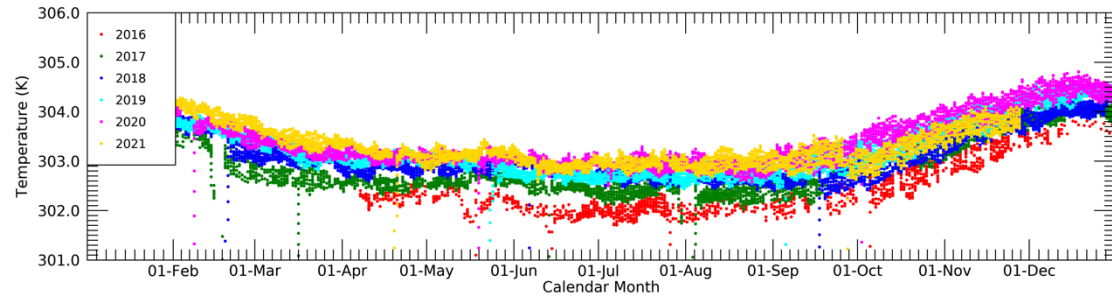
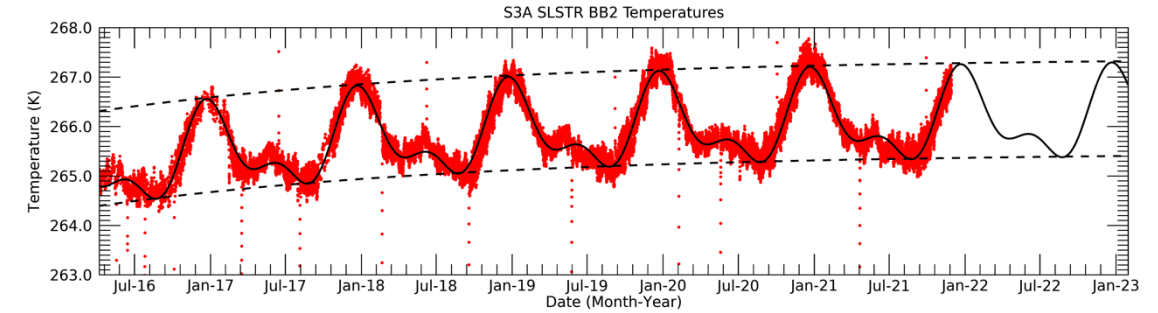
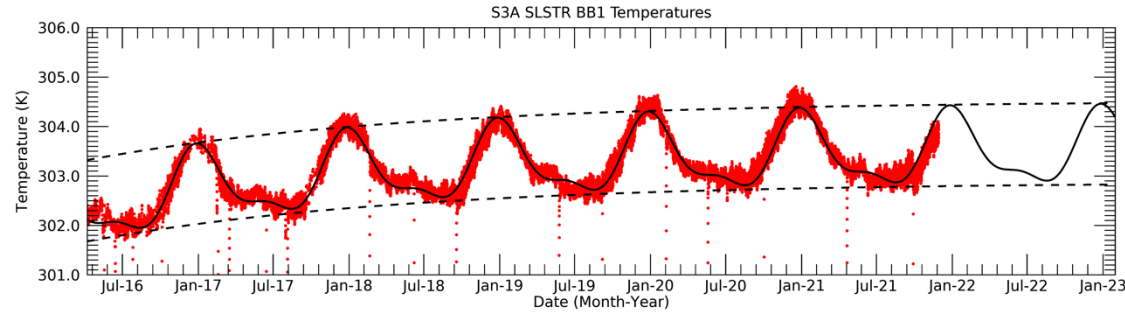
Seasonal variations – Sun-Earth distance + Earth Shine

Long term drift – due to ageing of thermal surfaces

- Temperature trend can be approximated by

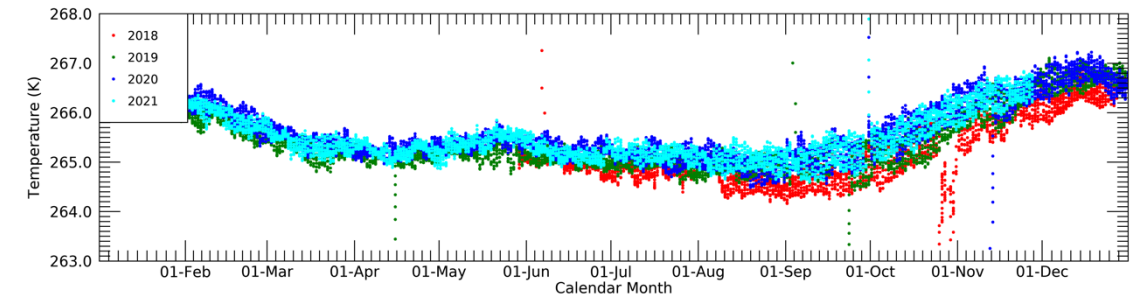
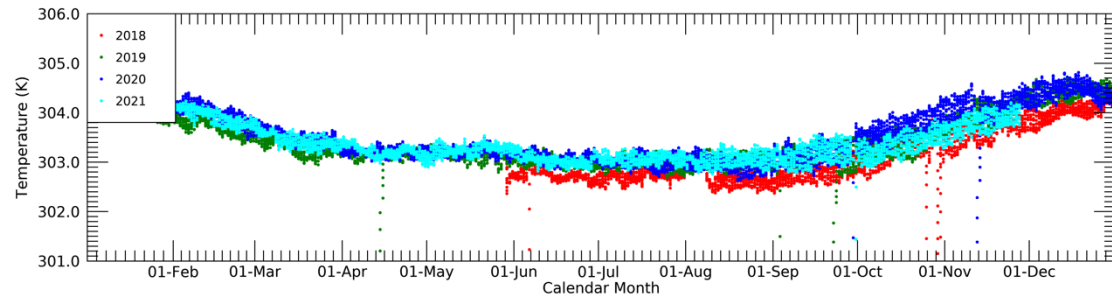
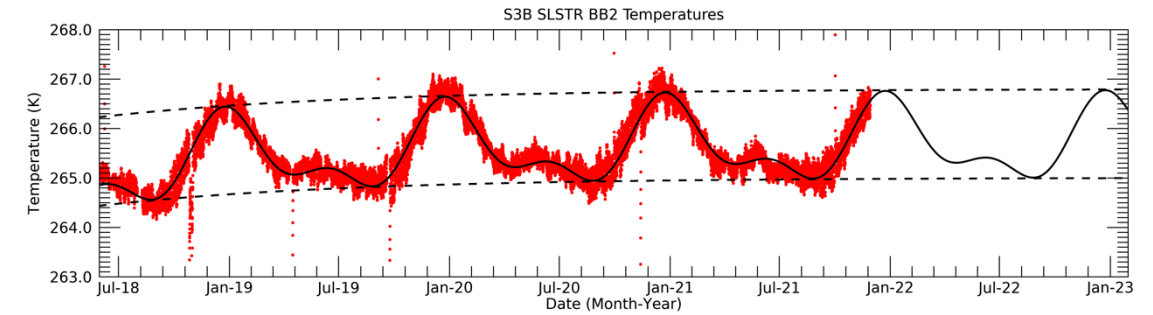
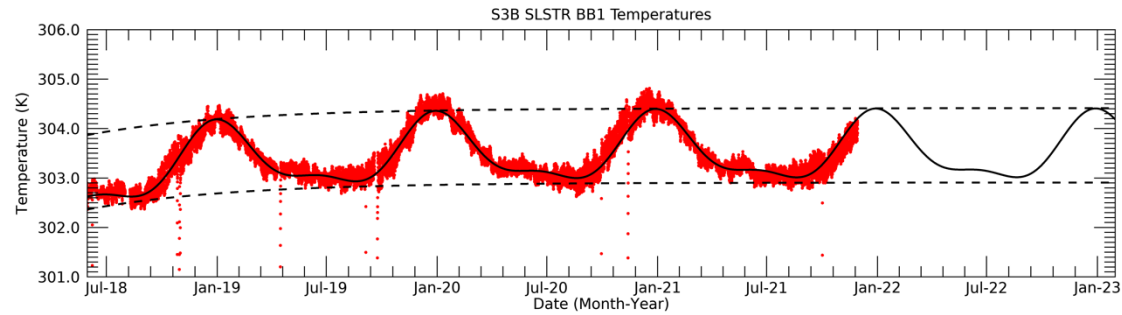
$$T(t) = T_0 + A_1 \cos(\theta(t) + \phi_1) + A_2 \cos(2\theta(t) + \phi_2) + A_3(1 - \exp(-kt))$$

SLSTR-A BB Temperatures



- Analysis predicts further ~ 0.20 K increase in BB temperatures by January 2025 – not accounting for reduction in heater power after BB cross-over test in September

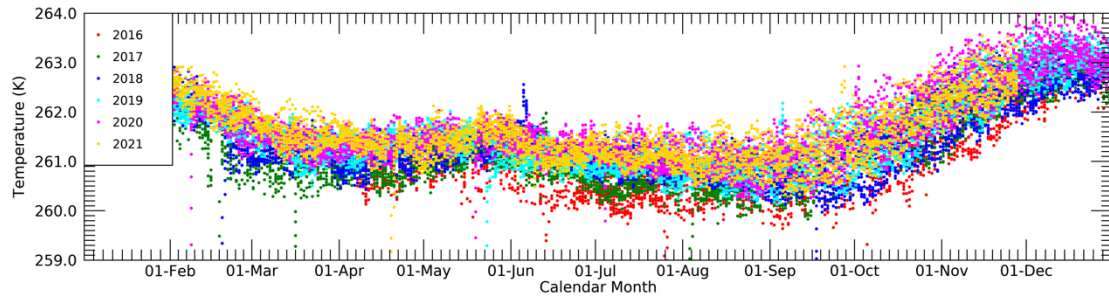
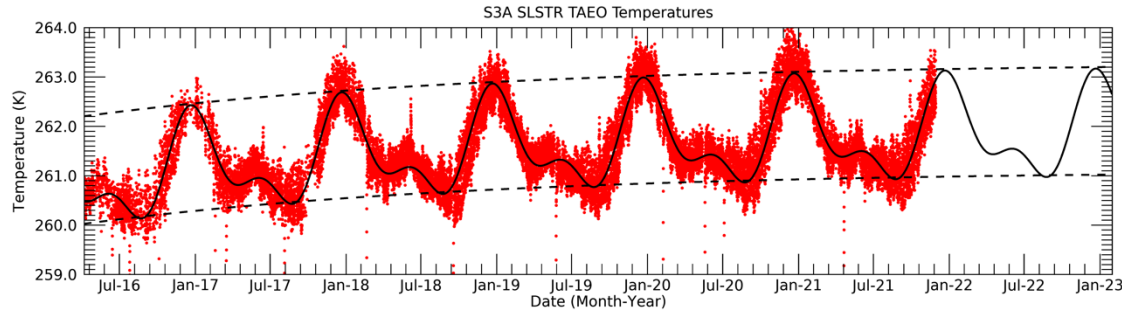
SLSTR-B BB Temperatures



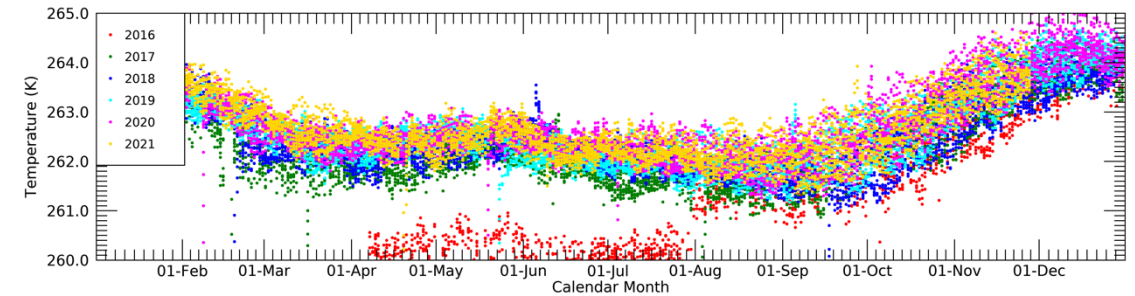
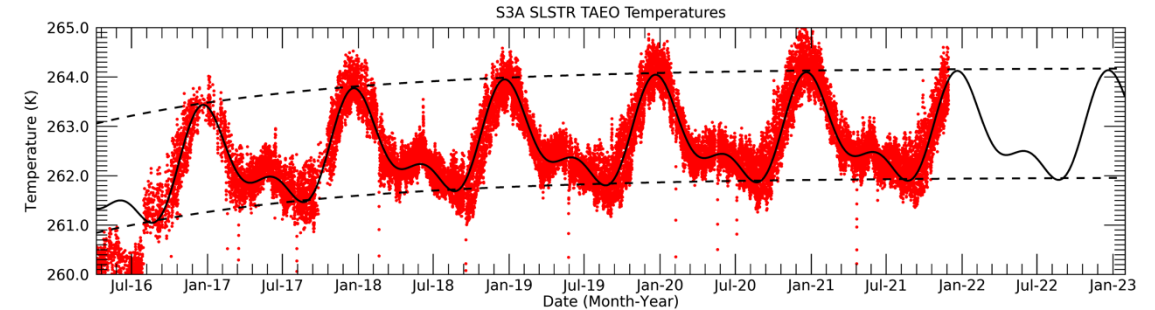
- Analysis predicts further ~ 0.55 K increase in BB temperatures by January 2025 – not accounting for reduction in heater power after BB cross-over test in September

SLSTR-A Paraboloid Mirror Temperatures

Nadir Mirror

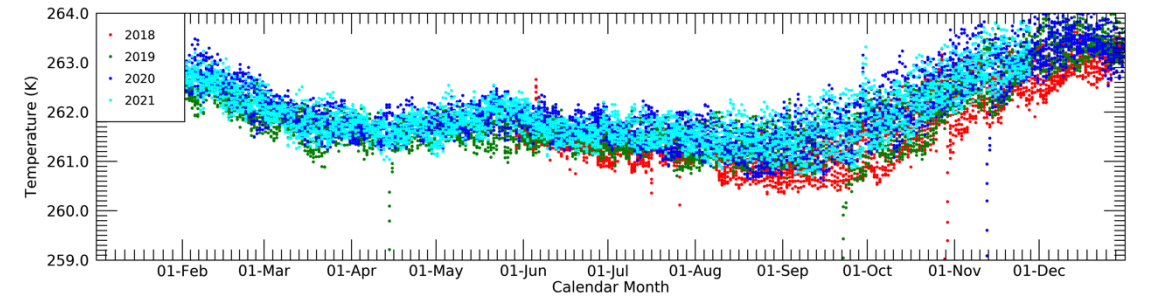
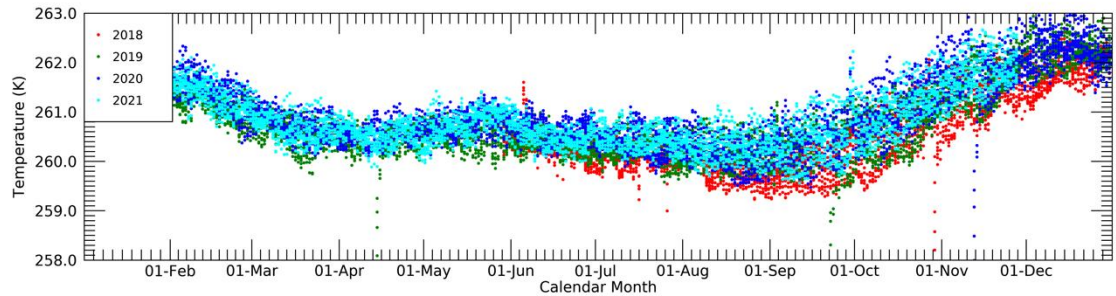
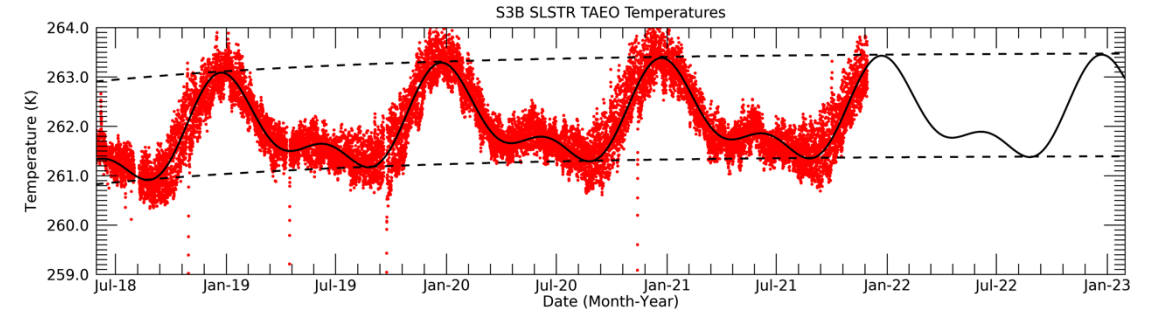
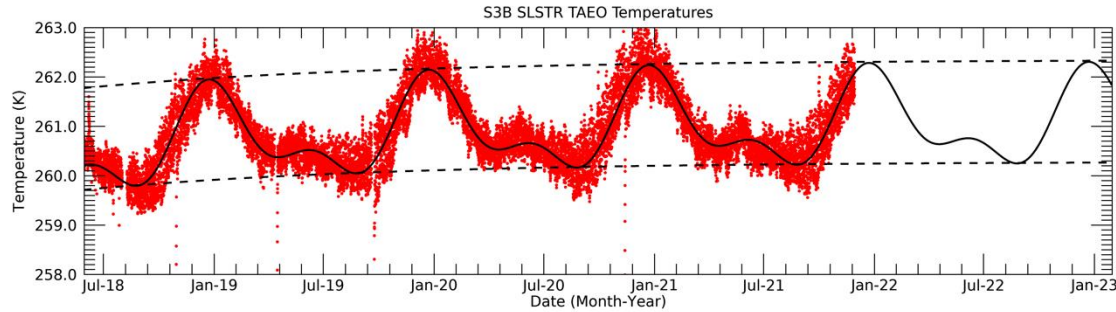


Oblique Mirror



- Analysis suggests OME temperatures are very stable - BUT may be biased by early temperature data

SLSTR-B Paraboloid Mirror Temperatures



- Analysis suggests OME temperatures are very stable

S3A Thermal Analysis

		2016	2017	2018	2019	2020	2021	2022	2023	2024	2025	2026
BB1	Max Temp (K)	303.86	304.18	304.38	304.5	304.58	304.62	304.65	304.67	304.68	304.69	304.69
	Rate (K/year)	0.4	0.25	0.16	0.1	0.06	0.04	0.02	0.01	0.01	0.01	0
BB2	Max Temp (K)	266.62	266.89	267.06	267.18	267.26	267.31	267.35	267.37	267.39	267.4	267.41
	Rate (K/year)	0.32	0.22	0.14	0.1	0.06	0.04	0.03	0.02	0.01	0.01	0.01
Nadir PMA	Max Temp (K)	262.44	262.69	262.87	262.99	263.07	263.13	263.17	263.19	263.21	263.22	263.23
	Rate (K/year)	0.31	0.21	0.15	0.1	0.07	0.05	0.03	0.02	0.02	0.01	0.01
Oblique PMA	Max Temp (K)	263.46	263.79	263.96	264.06	264.1	264.13	264.14	264.15	264.16	264.16	264.16
	Rate (K/year)	0.45	0.24	0.13	0.07	0.04	0.02	0.01	0.01	0	0	0
Flip Mirror Baffle	Max Temp (K)	267.87	268.14	268.32	268.44	268.52	268.58	268.62	268.64	268.66	268.67	268.68
	Rate (K/year)	0.32	0.22	0.15	0.1	0.07	0.05	0.03	0.02	0.01	0.01	0.01
Scan Mechanism	Max Temp (K)	270.99	271.4	271.65	271.81	271.91	271.97	272.01	272.04	272.05	272.06	272.07
	Rate (K/year)	0.51	0.32	0.2	0.13	0.08	0.05	0.03	0.02	0.01	0.01	0

S3B Thermal Analysis

		2018	2019	2020	2021	2022	2023	2024	2025	2026	2027	2028
BB1	Max Temp (K)	304.39	304.57	304.6	304.61	304.61	304.61	304.61	304.61	304.61	304.61	304.61
	Rate (K/year)	0.34	0.07	0.02	0	0	0	0	0	0	0	0
BB2	Max Temp (K)	266.52	266.72	266.8	266.83	266.85	266.85	266.85	266.86	266.86	266.86	266.86
	Rate (K/year)	0.3	0.12	0.05	0.02	0.01	0	0	0	0	0	0
Nadir PMA	Max Temp (K)	261.97	262.16	262.26	262.3	262.32	262.33	262.34	262.34	262.34	262.34	262.34
	Rate (K/year)	0.27	0.13	0.06	0.03	0.01	0.01	0	0	0	0	0
Oblique PMA	Max Temp (K)	263.11	263.3	263.4	263.44	263.46	263.47	263.48	263.48	263.48	263.48	263.48
	Rate (K/year)	0.28	0.13	0.06	0.03	0.01	0.01	0	0	0	0	0
Flip Mirror Baffle	Max Temp (K)	267.37	267.58	267.67	267.71	267.73	267.74	267.74	267.75	267.75	267.75	267.75
	Rate (K/year)	0.3	0.14	0.06	0.03	0.01	0.01	0	0	0	0	0
Scan Mechanism	Max Temp (K)	271.3	271.6	271.76	271.85	271.9	271.93	271.95	271.95	271.96	271.96	271.96
	Rate (K/year)	0.4	0.22	0.12	0.07	0.04	0.02	0.01	0.01	0	0	0

Uncertainty Estimates Update

- In 2019 we reported on the uncertainty analysis of the SLSTR-L1 uncertainties for TIR channels S7-S9
- Paper published in 2021 describing the status of the SLSTR level-1 traceability chain that links the uncertainty estimates to standards
 - e.g. temperature measurements.
- Uncertainty tools have been updated to incorporate into L0 monitoring to provide long term trends and to derive uncertainty estimates per orbit.



Article

Traceability of the Sentinel-3 SLSTR Level-1 Infrared Radiometric Processing

David Smith ^{1,*}, Samuel E. Hunt ², Mireya Etaluz ¹, Dan Peters ¹, Tim Nightingale ¹, Jonathan Mittaz ³, Emma R. Woolliams ² and Edward Polehampton ¹

¹ RAL Space, Science and Technology Facilities Council, Harwell, Oxford OX11 0QX, UK; Mireya.Etaluz@stfc.ac.uk (M.E.); daniel.peters@stfc.ac.uk (D.P.); Tim.Nightingale@stfc.ac.uk (T.N.); edward.polehampton@stfc.ac.uk (E.P.)

² National Physical Laboratory, Teddington TW11 0LW, UK; Sam.Hunt@npl.co.uk (S.E.H.); emma.woolliams@npl.co.uk (E.R.W.)

³ Department of Meteorology, University of Reading, Reading RG6 6AL, UK; j.mittaz@reading.ac.uk

* Correspondence: dave.smith@stfc.ac.uk; Tel: +44-1235-445996

Abstract: Providing uncertainties in satellite datasets used for Earth observation can be a daunting prospect because of the many processing stages and input data required to convert raw detector counts to calibrated radiances. The Sea and Land Surface Temperature Radiometer (SLSTR) was designed to provide measurements of the Earth's surface for operational and climate applications. In this paper the authors describe the traceability chain and derivation of uncertainty estimates for the thermal infrared channel radiometry. Starting from the instrument model, the contributing input quantities are identified to build up an uncertainty effects tree. The characterisation of each input effect is described, and uncertainty estimates provided which are used to derive the combined uncertainties as a function of scene temperature. The SLSTR Level-1 data products provide uncertainty estimates for fully random effects (noise) and systematic effects that can be mapped for each image pixel, examples of which are shown.

Keywords: calibration; uncertainty; traceability; SLSTR; Sentinel-3; temperature; blackbody; radiometer; data processing; Earth observation; metrology



Citation: Smith, D.; Hunt, S.E.; Etaluz, M.; Peters, D.; Nightingale, T.; Mittaz, J.; Woolliams, E.R.; Polehampton, E. Traceability of the Sentinel-3 SLSTR Level-1 Infrared Radiometric Processing. *Remote Sens.* **2021**, *13*, 374. <https://doi.org/10.3390/rs13030374>

Academic Editor: Adam Povey
Received: 14 December 2020
Accepted: 16 January 2021
Published: 22 January 2021

Publisher's Note: MDPI stays neutral with regard to jurisdictional claims in published maps and institutional affiliations.



Copyright: © 2021 by the authors. Licensee MDPI, Basel, Switzerland. This article is an open access article distributed under the terms and conditions of the Creative Commons Attribution (CC BY) license (<https://creativecommons.org/licenses/by/4.0/>).

1. Introduction

Satellite datasets used for Earth observation and climate research need an indication of quality to allow users to assess the suitability of the data for their particular application [1]. At the most basic level, the quality of a measurement is defined in terms of its uncertainty and traceability to standard references. The processing of raw satellite data (Level-0 data) to radiometrically calibrated and geo-referenced data products (Level-1 data) involves a number of stages and relies on several auxiliary data files (ADFs) that contain calibration coefficients and tables used for converting digital counts to physical quantities [2]. These coefficients are derived from characterization measurements of different components of the instrument system. Furthermore, the derivation of the calibration source radiances is dependent not just on a single parameter, e.g., a temperature measurement, but other input quantities such as thermal gradients. Thus, the uncertainty of the data products is dependent on all effects contributing to the data processing. Furthermore, the uncertainty associated with a single observation in a single pixel is unlikely to be a single value but can vary with scene radiance.

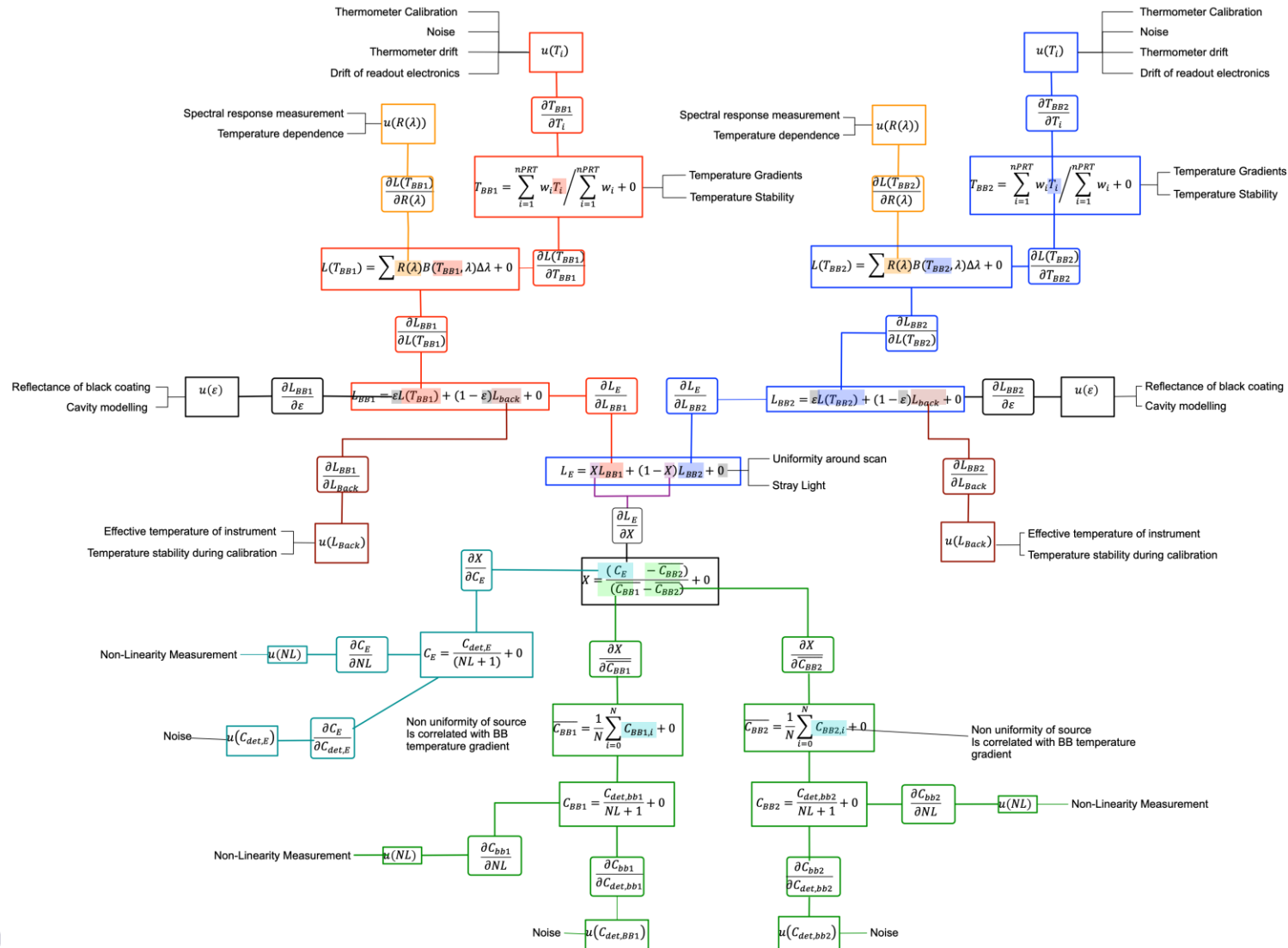
The Sea and Land Surface Temperature Radiometer (SLSTR) on the Copernicus Sentinel-3 mission is an instrument designed to retrieve global sea surface temperatures (SSTs) for climate monitoring [3]. Two satellites (model A and B) provide near complete daily global coverage. SLSTR is a development of the along-track scanning radiometer series [4] and shares many of the key design features [5] needed for accurate measurement

Remote Sens. **2021**, *13*, 374. <https://doi.org/10.3390/rs13030374>

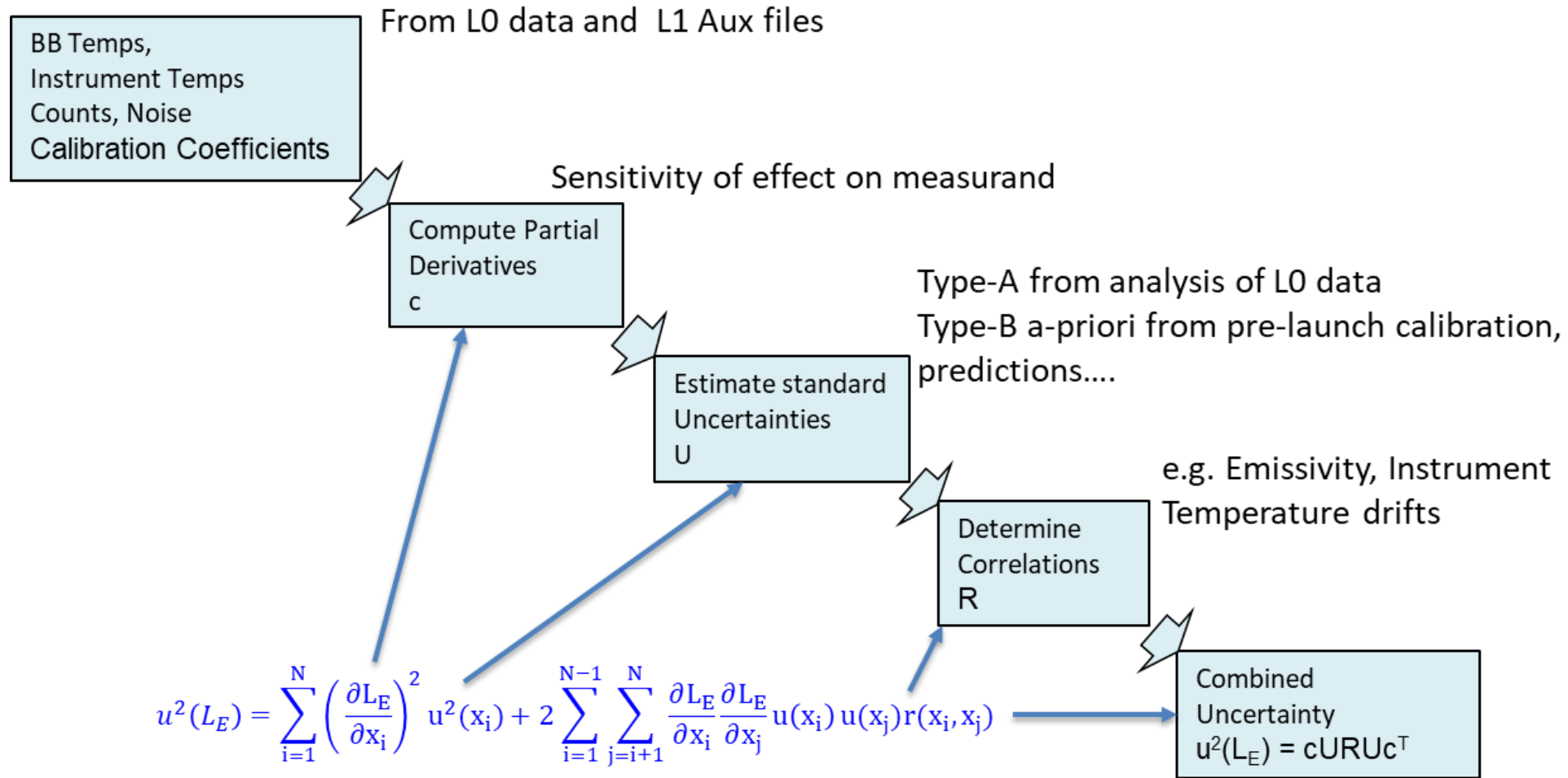
<https://www.mdpi.com/journal/remotesensing>

<https://doi.org/10.3390/rs13030374>

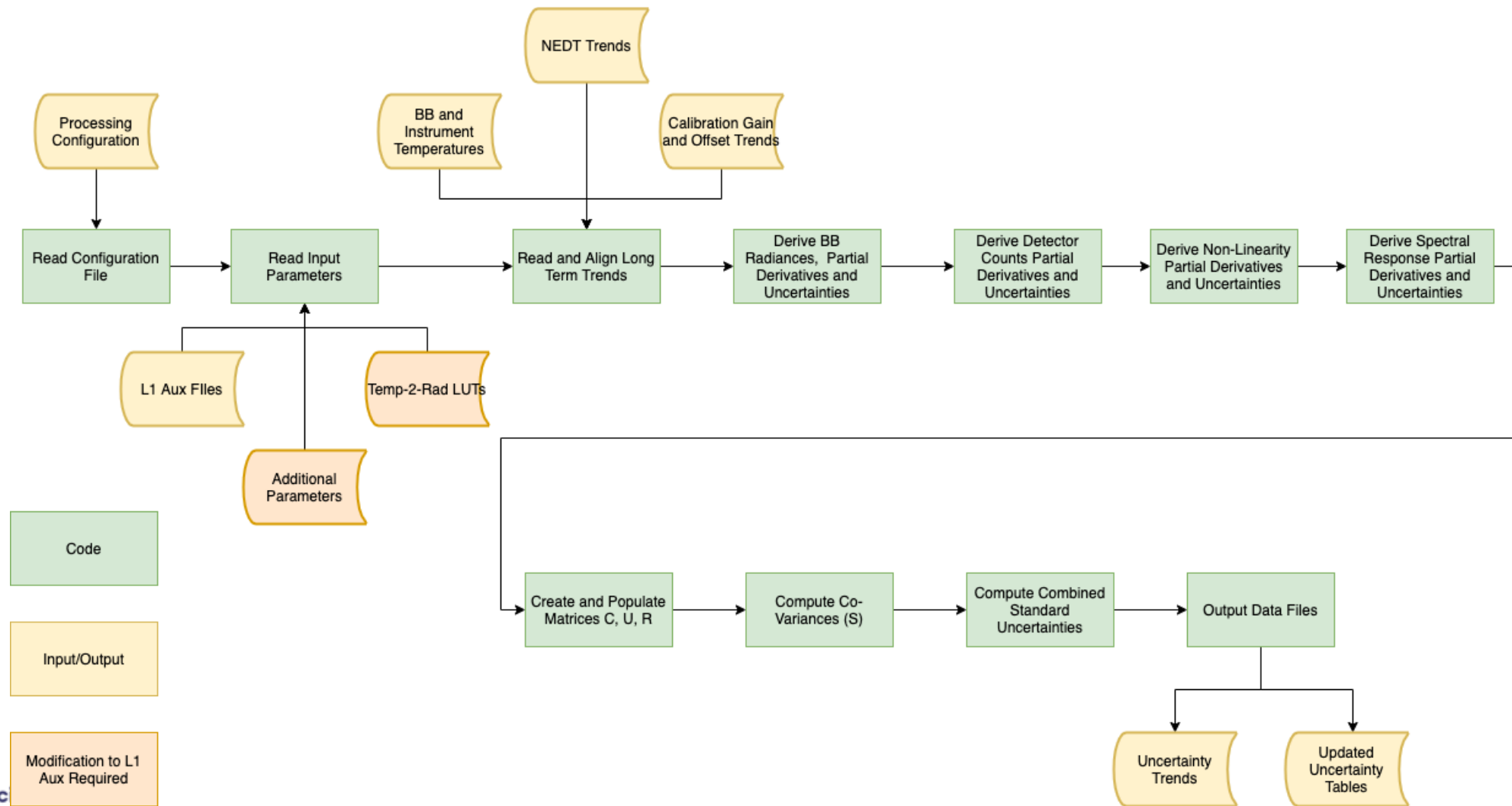
SLSTR TIR Calibration – Traceability Chain



Deriving L1 Uncertainties from L0

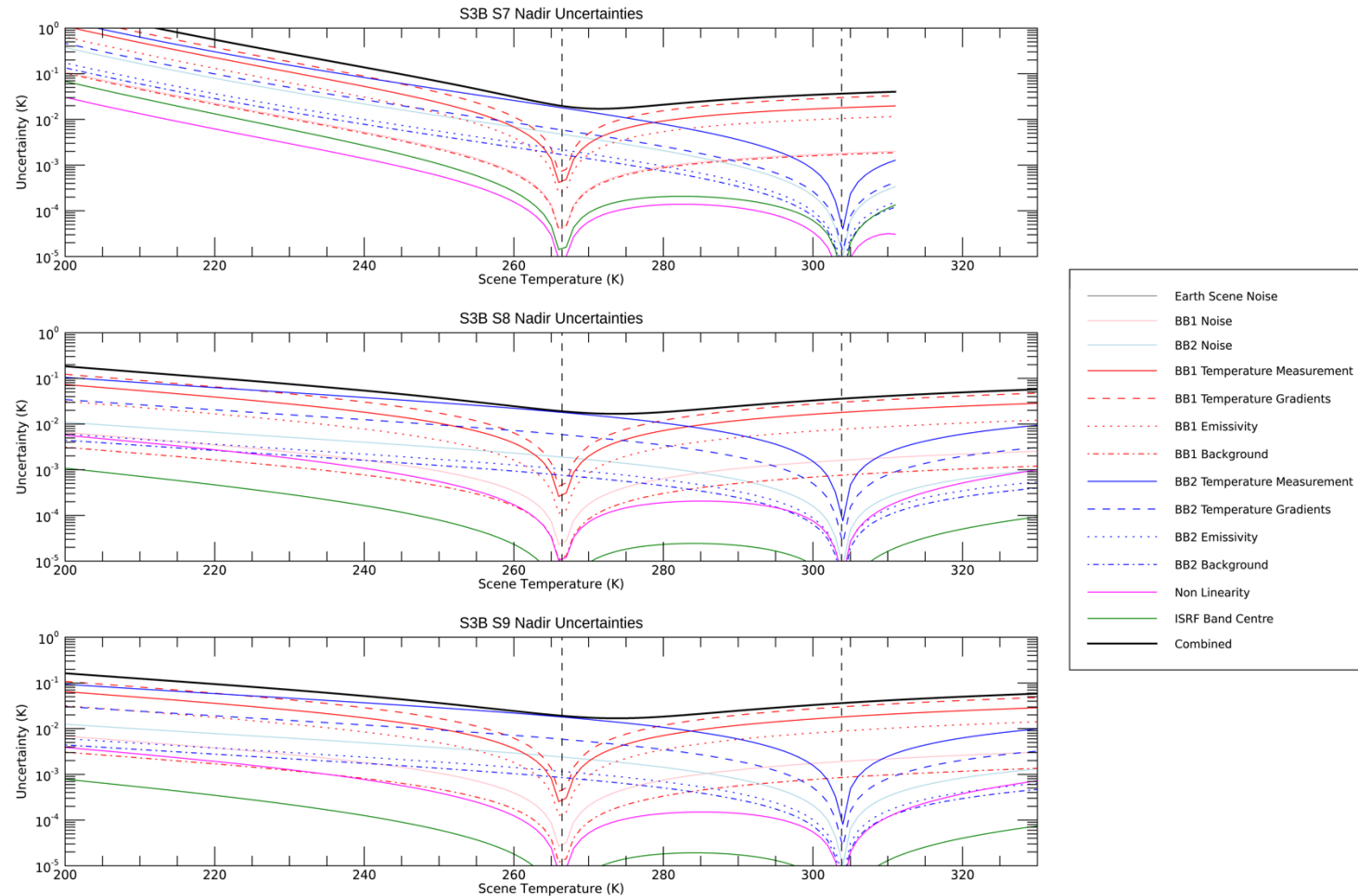


Uncertainty Tool – Processing Chain



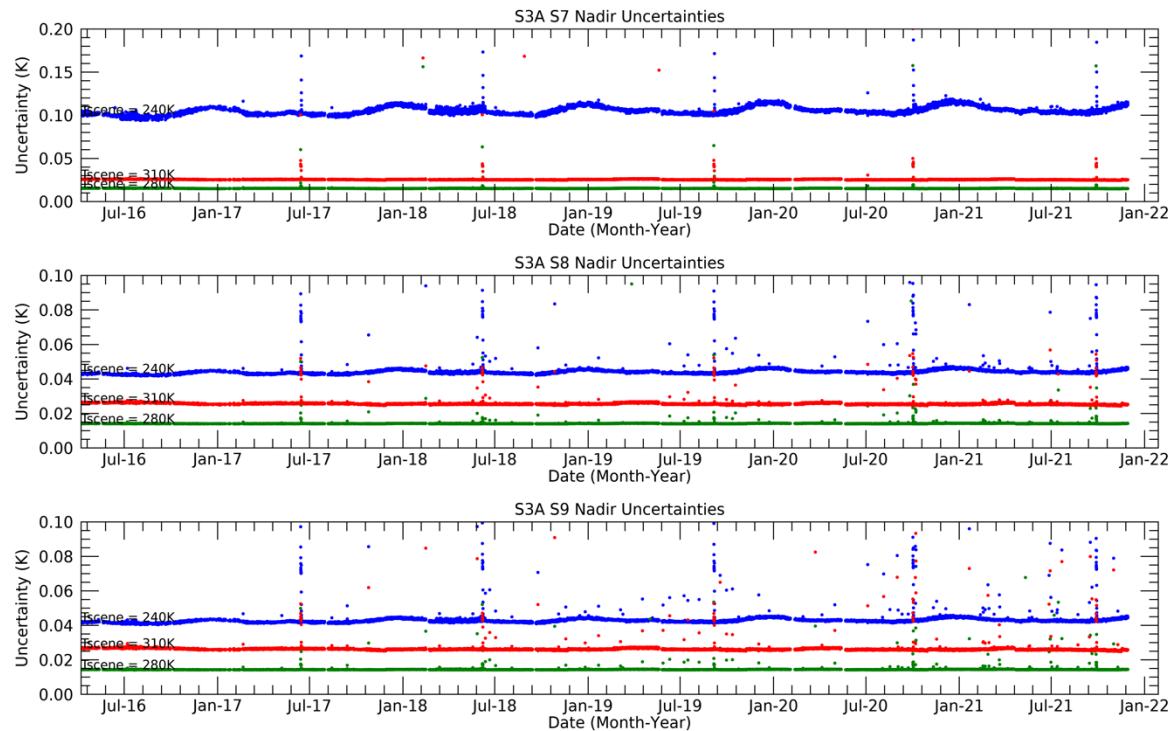
SLSTR Uncertainty Budget

- Black-Body Temperatures
 - PRT calibration at subsystem level – traced to SPRT (ITS-90) – NPL/NIST
 - Blackbody gradients, thermal analysis - RAL
- Black-Body Cavity Emissivity
 - Spectral Reflectance of Black Coating – NIST/NPL
 - Cavity Model – STEEP323 or SMART3D (ABSL model)
- Spectral Response
 - FPA measurements – RAL reports [S3-RP-RAL-SL-102 (S3A), S3-RP-RAL-SL-114 (S3B)]
- Non-Linearity
 - Instrument level calibration tests – RAL reports
- Detector Noise
 - Instrument level calibration tests, on-board BB sources

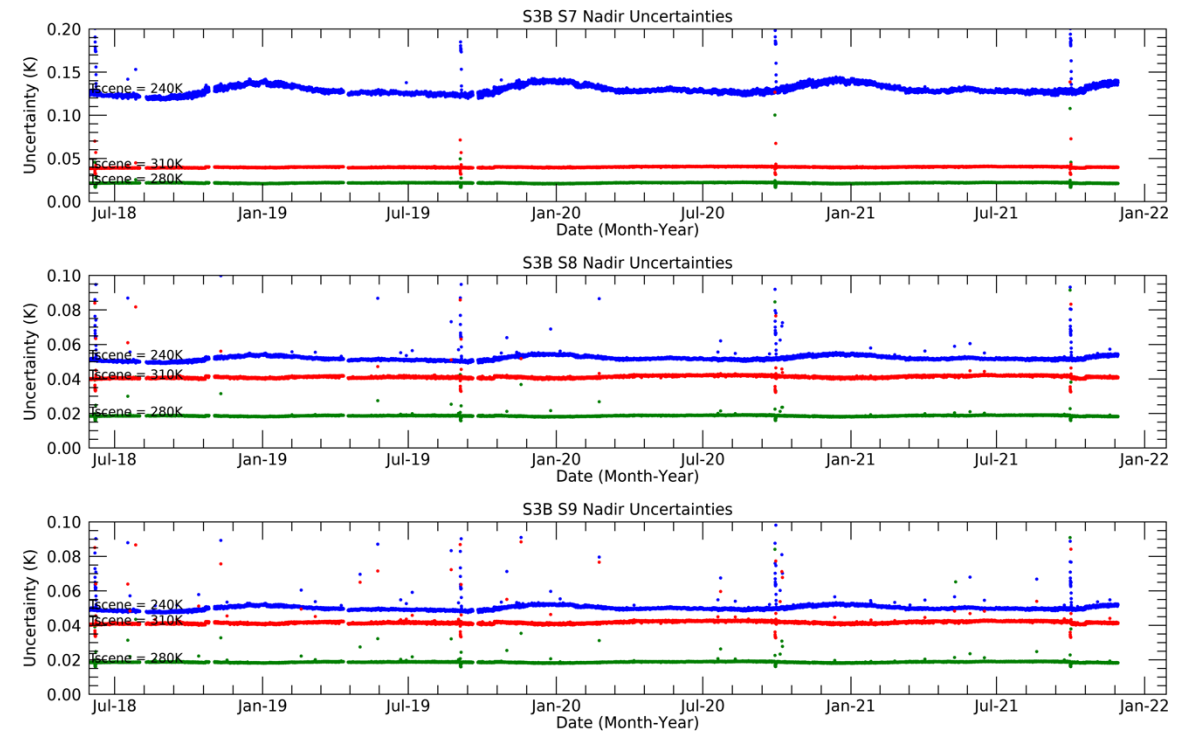


Uncertainty Time Series - Correlated Effects

SLSTR-A



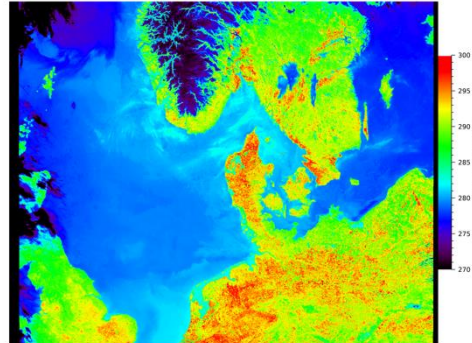
SLSTR-B



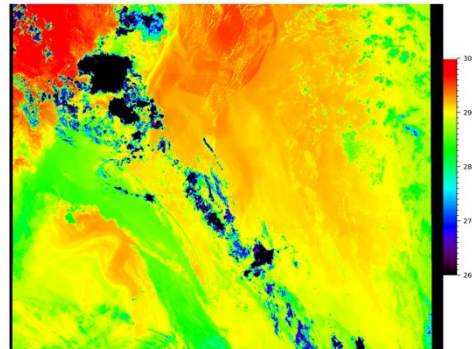
Uncertainties in SLSTR L1 Products

- Random effects - detector noise expressed as NEDT (TIR channels) and NEDL (VIS/SWIR channels) for each scan line
- Systematic effects – radiometric calibration - tables of uncertainty vs. temperature type-B (a-priori) estimates based on the pre-launch calibration and calibration model
- MapnoiS3 tool developed by RAL allows mapping of uncertainty information to L1 images

12um
BT

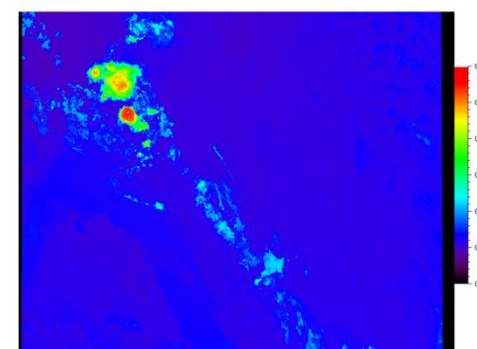


North Sea on 22-April-2020

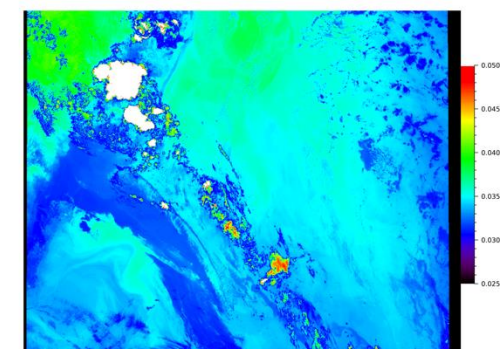
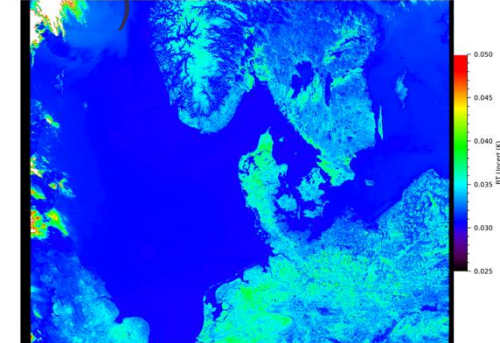


Australia on 01-Jan-2020

12um NEDT
(Random)




12um uBT
(Systematic)



Images from Smith D. et al, **Traceability of the Sentinel-3 SLSTR Level-1 Infrared Radiometric Processing**, Remote Sens. 2021, 13(3), 374; <https://doi.org/10.3390/rs13030374>

MapnoiS3 v2.0. Updates

- MapNoiS3 v1.0
 - Radiometric uncertainties: Estimates of the correlated effects derived from the pre-launch calibration are provided in the Level-1 quality datasets.
 - MapNoiS3 v2.0
 - Uncertainty estimates are derived from the Level-0 monitoring tool and are available as a separate source.
 - Radiometric uncertainties per orbit as function of scene temperature LUT in NetCDF files.
 - S3A_SL_20211011T214456_TIR_Uncerts.nc
- 
<orbit_mean_date>
- **Updates:**
 1. The user can select the data source to map the radiometric uncertainties to the L1 data.
 2. Scaling factors to integer NEDT for TIR channels were modified in order to cover the NEDT negative values obtained at the lowest BT.
 3. The tool has been implemented to account for the rename of the Fire channels products. It can read F1_..._in.nc and F1_..._fn.nc products.

MapnoiS3 implementation

```
<?xml version="1.0" encoding="UTF-8"?>
<mapnoiS3_config>
  <path_slstr      value="/data/" description="Path to SLSTR L1 input products" type="STRING" />
  <path_adfL1     value="/mapnoiS3_20211130/input/ADFs/Level1/" description="Path to SLSTR ADF L1 input products" type="STRING" />
  <path_adfL2     value="/mapnoiS3_20211130/input/ADFs/Level2/" description="Path to SLSTR ADF L2 input products" type="STRING" />
  <channels       value="s1,s3,s6,s7,s8,f1,f2" description="List of channels to process, separated by commas" type="STRING" />
  <scan          value="nadir,oblique" description="Scan view to process (nadir and/or oblique, separated by comma)" type="STRING" />
  <path_out       value="/mapnoiS3_20211130/output/" description="Path to output products" type="STRING" />
  <select_uncert  value="orbit" description="Select the radiometric uncertainties LUT: 'orbit' (for the L1 combined uncertainties), or 'ground' (for quality products)" type="STRING" />
  <path_tir_uncerts value="/tir_uncerts/" description="Path to SLSTR L1 tir uncertainty products" type="STRING" />
</mapnoiS3_config>
```

- **Selection of Radiometric Uncertainties LUT as a function of scene temperature:**

<select_uncert> { Value= "ground" Radiometric uncertainties LUT is taken from the Level-1 quality products
Value= "orbit" Radiometric uncertainties LUT is acquired from the external Level-1 uncertainty netCDF files

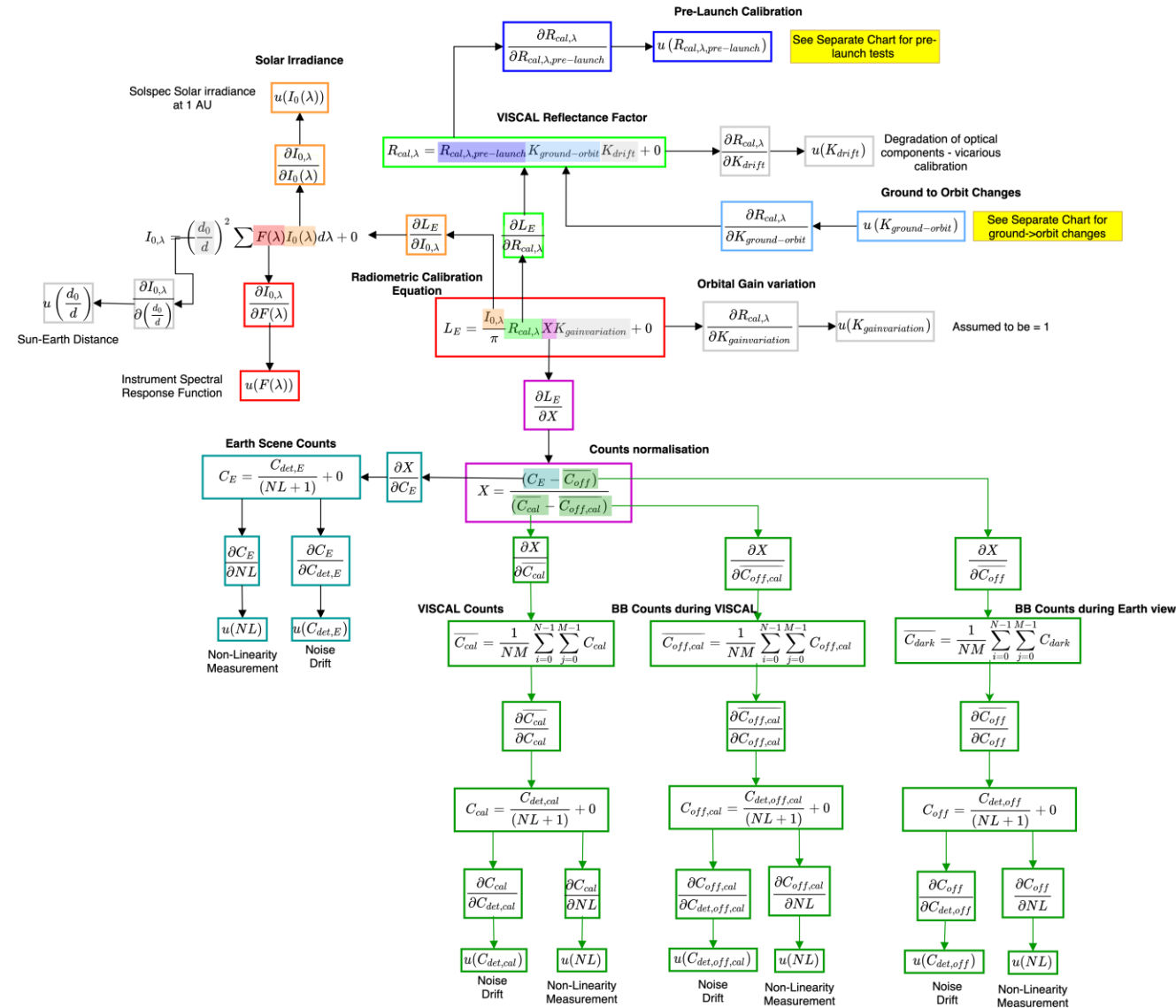
<path_tir_uncerts> Path to the Level-1 uncertainty netCDF files

If **<select_uncert>** Value= "orbit" then:

- MapnoiS3 looks for Level-1 uncertainty netCDF files in **<path_tir_uncerts>**
- For each SLSTR Level-1 product **<start_time>**, it takes the uncertainty .nc such as **|<orbit_mean_date> - <start_time>|**= minimum
- If **|<orbit_mean_date> - <start_time>| > 50 minutes**, then:
 - MapnoiS3 warns the user that the Level-1 uncertainty netCDF file doesn't belong to the orbit of the SLSTR L1 product.
 - MapnoiS3 asks the users weather they want to use the Level-1 uncertainties or the quality product instead.

Future Developments

- Analysis has focused on TIR channels as these are the primary mission.
- For VIS/SWIR channels MapNoiS3 uses uncertainties in L1 Quality datasets based on pre-launch analysis.
- Future development would be to perform similar analysis for VIS/SWIR channels considering in-flight performance



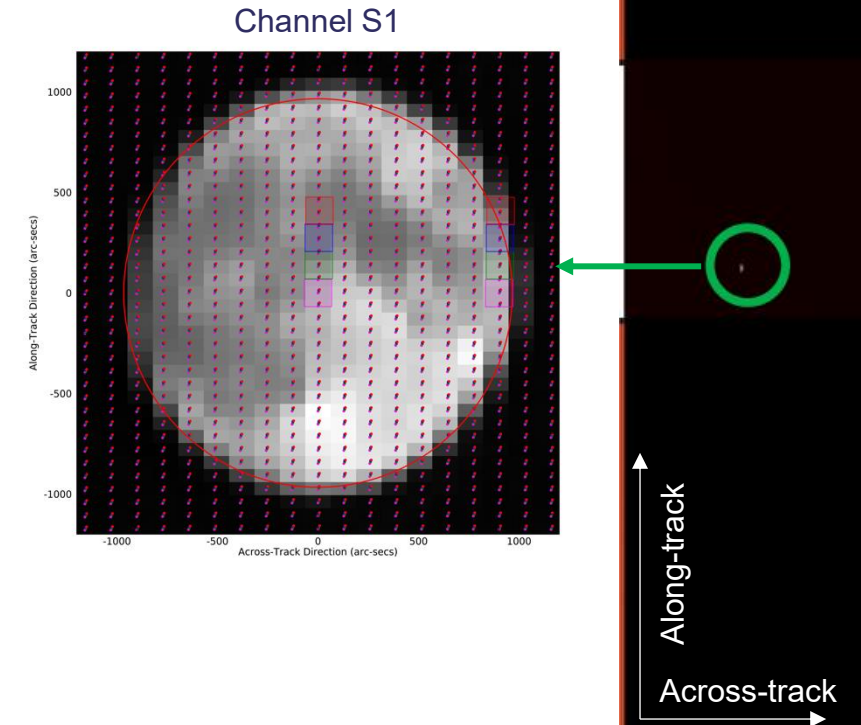
Lunar Irradiance Calibration

- Many satellite instruments used for earth observation are using Lunar observations to provide a calibration reference for the VIS-SWIR range.
- This is facilitated by accurate Lunar irradiance models derived from ground based radiometric observations of the moon.
- ROLO (RObotic Lunar Observatory) – USGS Field Station, Flagstaff Az (Tom Stone)
 - GIRO is the GSICS implementation of ROLO
 - Thomas C. Stone, "Radiometric Calibration Stability and Inter-calibration of Solar-band Instruments in Orbit Using the Moon," Proc. SPIE 7081 70810X-1-8 (2008)
- LIME (Lunar Irradiance Model ESA) – Derived from measurements performed at Pico Teide in Tenerife (Spain)
 - Led by NPL (UK) in collaboration with the University of Valladolid (Spain) and the Flemish Institute for Technological Research (VITO) (Belgium).
 - <http://calvalportal.ceos.org/lime>
- Models provide integrated at sensor Lunar Irradiance spectra corrected for Lunar phase angle and distance to Sun and Spacecraft.



SLSTR Lunar Observations

- Observations of the moon by Sentinel-3 were performed after a roll manoeuvre with the satellite in a stable orientation.
 - S3B SLSTR observation was made on 27/07/2018 at ~5:20 UTC
 - S3A SLSTR observation was made on 04/07/2020 at ~16:10 UTC
 - Very similar lunar phase : -6.46deg (S3B) vs -6.29deg (S3A)
- SLSTR observed the Moon in nadir view with all the channels: the VIS (S1-S3), the SWIR (S4-S6) and the TIR (S7-S9).
- The manoeuvres also allowed observations of the cold sky to verify the dark signals of the VIS-SWIR channels and provide an additional low-temperature calibration point using the channels S8 and S9.



Moon – 04-07-2020 – S3A



Time Saturday, July 04, 2020, 16:00 UT

Phase 99.7% (13d 9h 19m)

Diameter 1900.4 arcseconds

Distance 377139 km (29.60 Earth diameters)

J2000 Right Ascension, Declination 18h 26m 49s, -23° 57' 44"

Subsolar Longitude, Latitude 11.368°, 0.425°

Sub-Earth Longitude, Latitude 4.653°, 0.916°

Position Angle 355.822°

Moon – 27-07-2018 – S3B



Time Friday, July 27, 2018, 05:00 UT

Phase 99.6% (14d 2h 12m)

Diameter 1764.3 arcseconds

Distance 406228 km (31.88 Earth diameters)

J2000 Right Ascension, Declination 19h 55m 19s, -19° 58' 43"

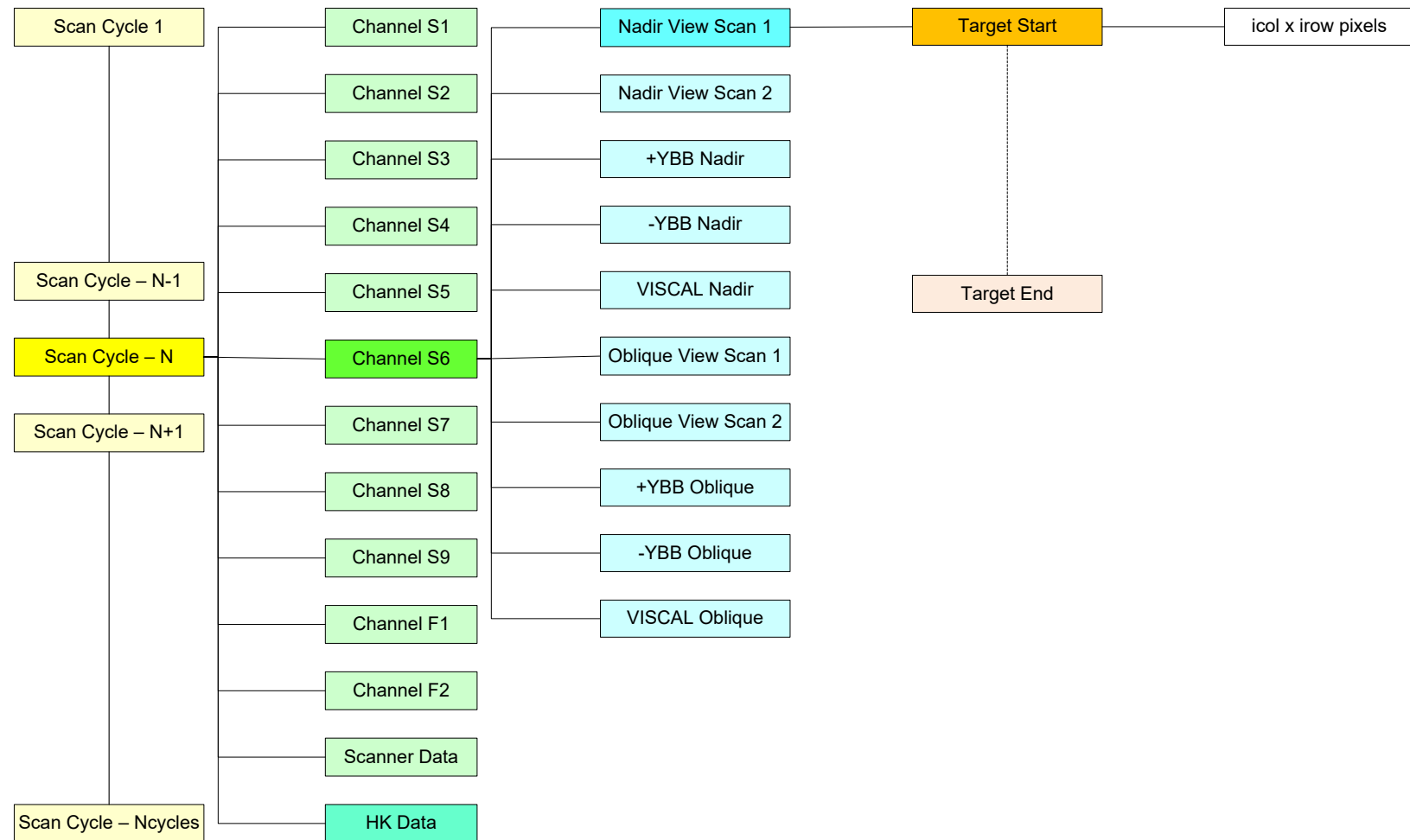
Subsolar Longitude, Latitude 7.324°, -0.051°

Sub-Earth Longitude, Latitude 0.438°, -1.037°

Position Angle 347.398

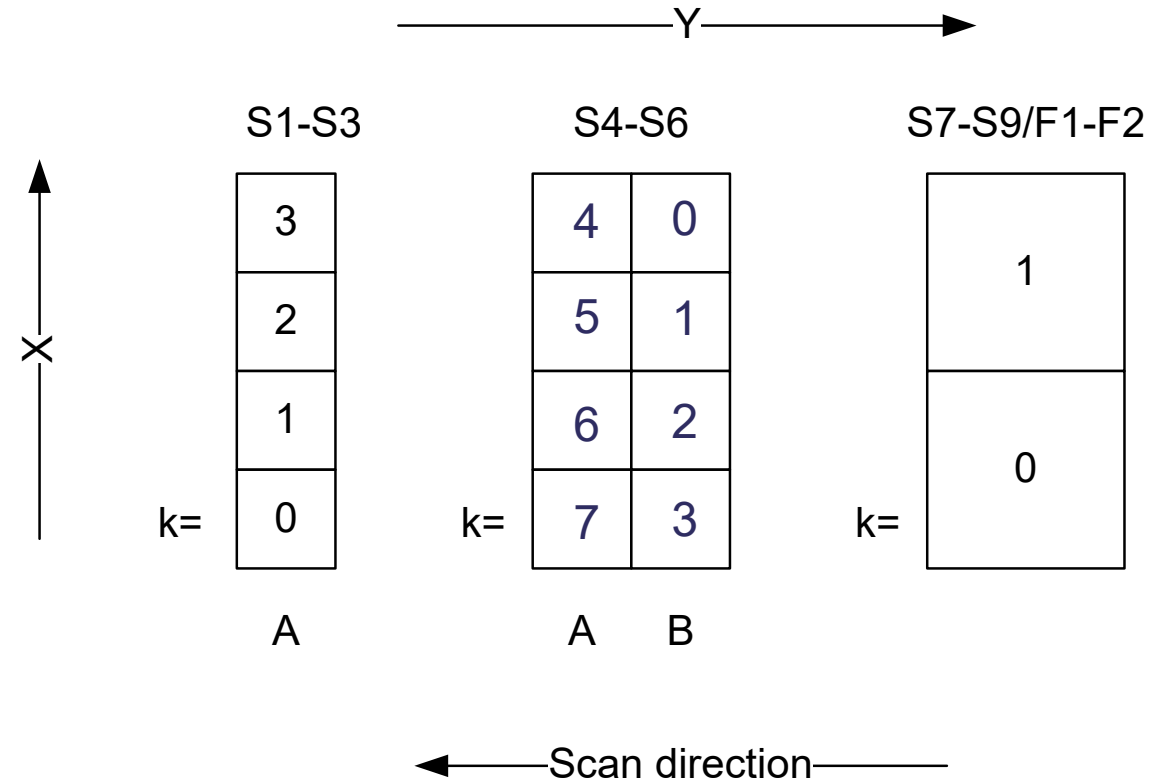
SLSTR L0 Data Structure

- For each scan cycle, L0 data contains packets for each channel and each view.
- Each view packet contains each detector counts for each pixel in the view.



Detector Ordering

- Note detectors read-out order is not conveniently in their optical position.
- E.g. In L0 data, SWIR detector corresponding to VIS detector 0 is read out last.
- We need to swap the order of the SWIR detectors so that they are aligned to the VIS channels.



Conversion to Radiances

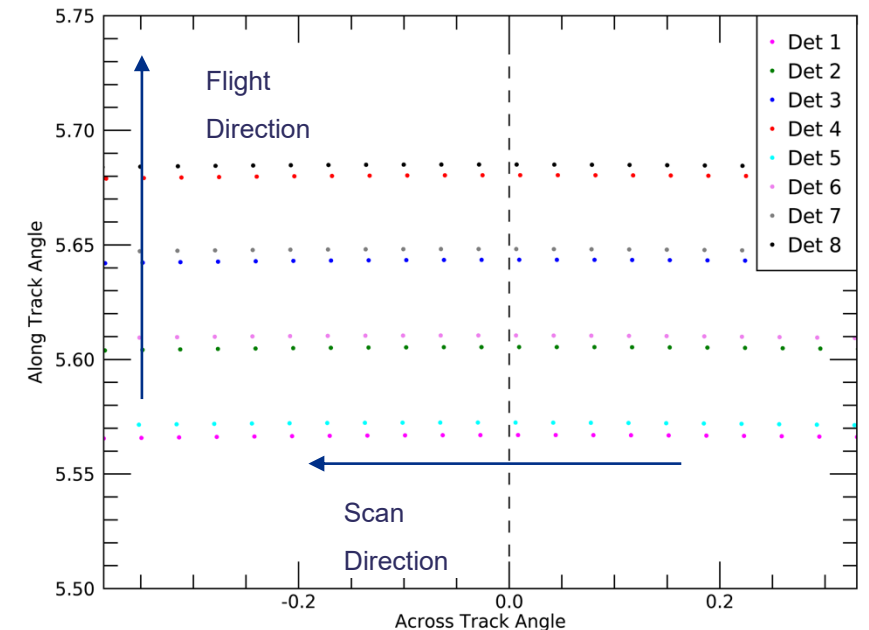
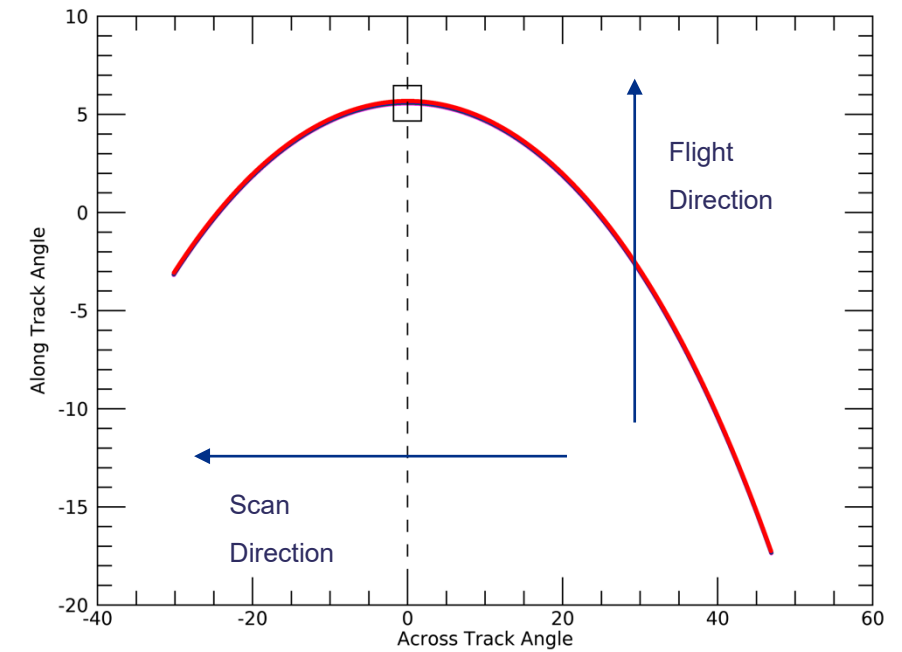
- From L0 packets we extract the nadir view detector counts for each channel
 - We get a matrix `L0_Counts`, of dimensions – `ndets`, `npixels`, `nscans`
- Apply non-linearity correction using L1 auxiliary files
 - `L0_Counts_corrected = L0_Counts / (NL+1)`
- Convert to reflectance using BB counts and Cal-Slope in VISCAL auxiliary file
 - `Reflectance = (L0_counts_corrected - BB_counts) * Cal_Slope`
- Convert to radiance using Solar Irradiance in VISCAL auxiliary file
 - `Reflectance = Reflectance * Solar_Irradiance / pi`

Geometric Calibration

- To map the moon pixels to the sky we need to consider the conical scanning geometry of the instrument.
- Pixel line-of-sight is determined using the instrument geometric model described in the L1 ATBD.

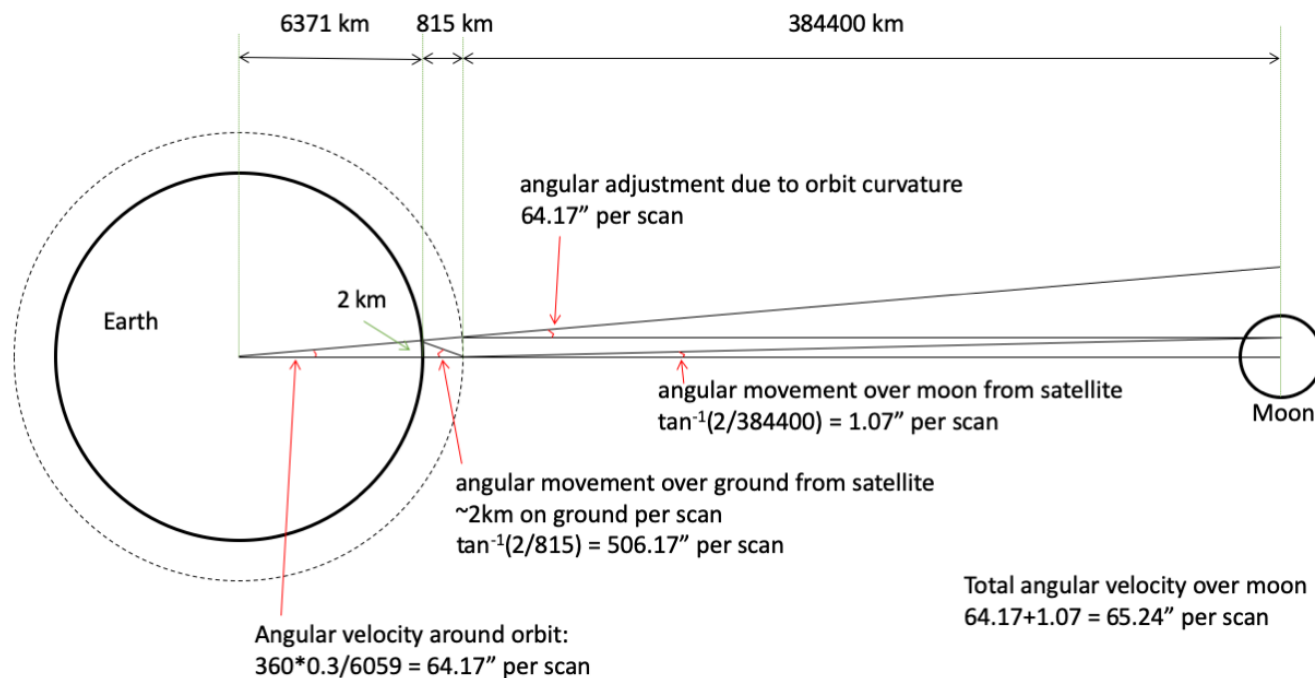
$$M_{ab}^v M_{los_{grid}}'^v = M_{ab}^v M_{ac}^{-1} M_{cm}^{v-1} \begin{pmatrix} -1 & 0 & 0 \\ 0 & -1 & 0 \\ 0 & 0 & 1 \end{pmatrix} M_{cm}^v M_{ac} M_{los_{grid}}^v$$

- However, the Moon is present only in the centre of the scan so occupies only a view pixels where the direction of the scan is only across-track.
- Hence only spacing between pixels is necessary. Absolute position is not critical.



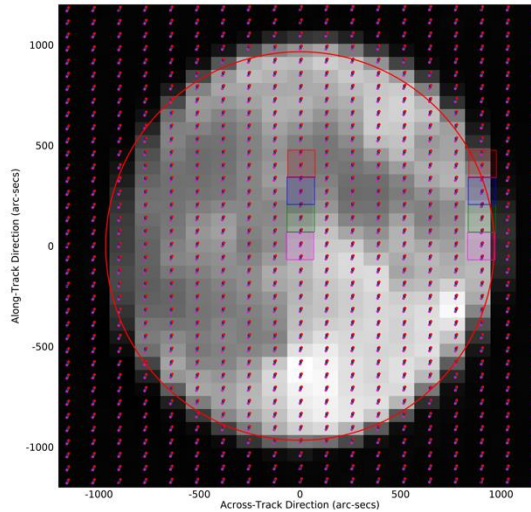
Pixel Spacing

- Across track distance between pixels is determined by scan geometry and time between pixel samples (40us).
 - Across track interval on moon = 127.742" (For S1-S6)
- Along track distance is determined by motion of satellite + scan interval
 - Along track interval on moon = 65.25"

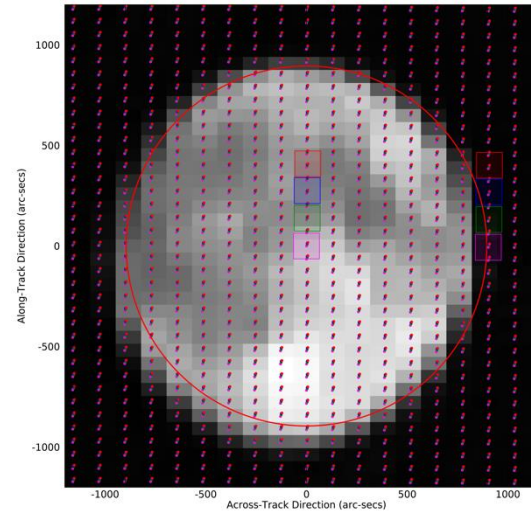


Lunar Mapping

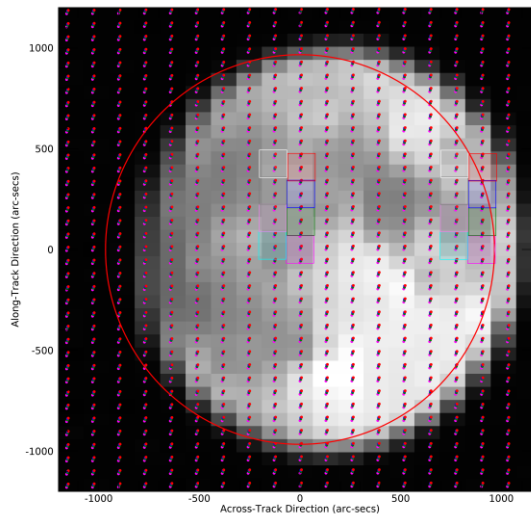
S3A – Channel S1



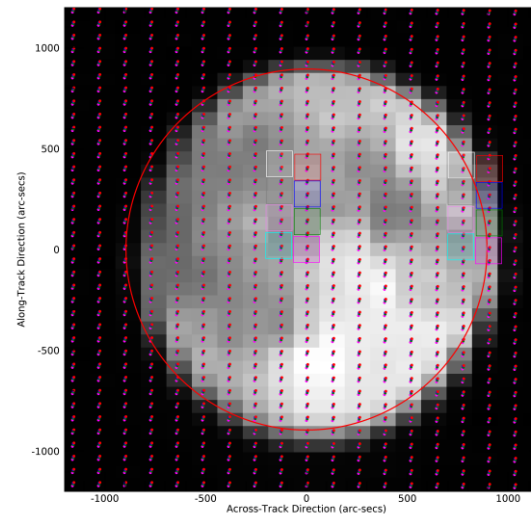
S3B – Channel S1



S3A – Channel S6



S3B – Channel S6



Points show relative position of detector centres based on LoS measurements & LoS model.

Squares show effective area of detector footprint projected onto sky.

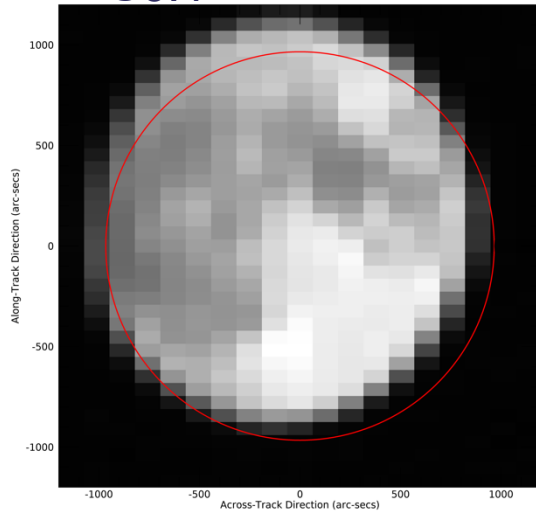
Circle shows size of moon disc as viewed from spacecraft.

Note S3B lunar image is smaller than S3A – due to differences in distance from satellite to moon.

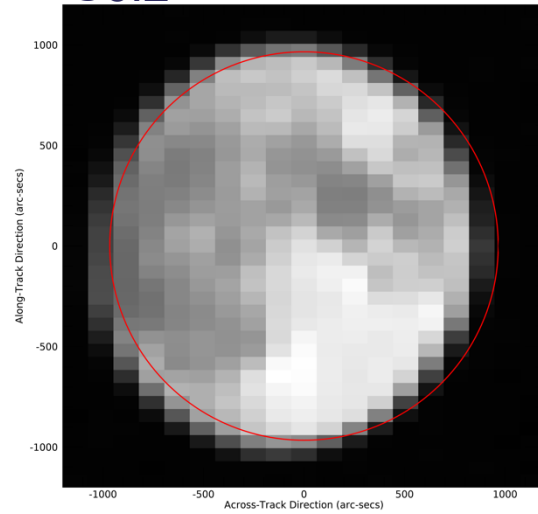
Note also difference in moon across-track position between S6 and S1 detectors

Moon in Different Detectors – SLSTR-A Channel S6

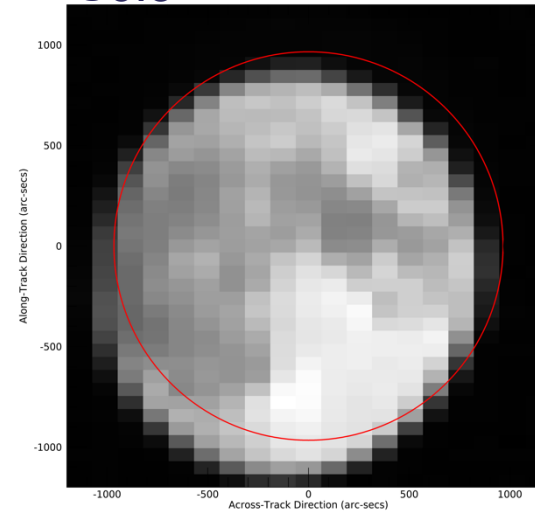
S6.1



S6.2

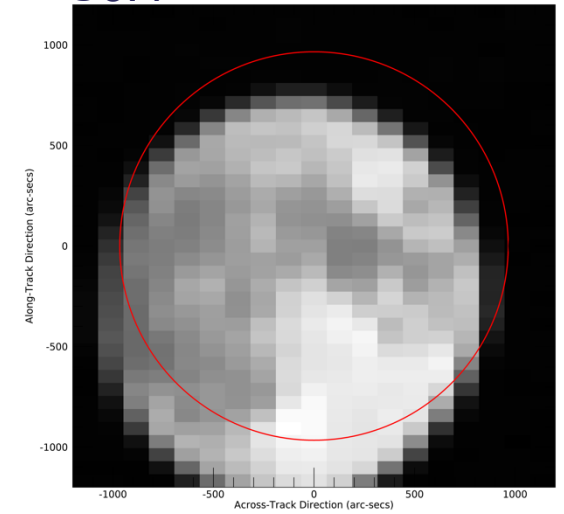


S6.3

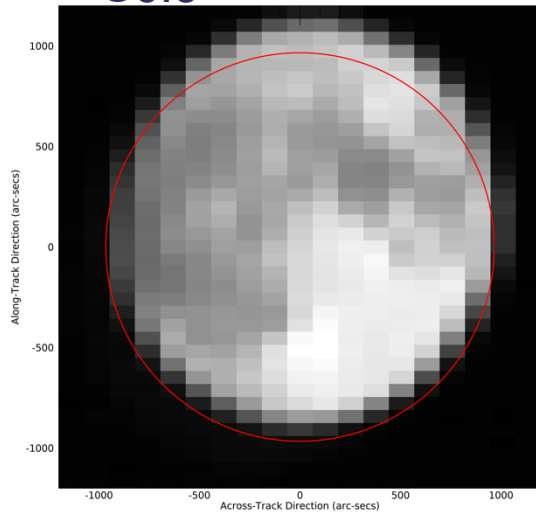


S6.4

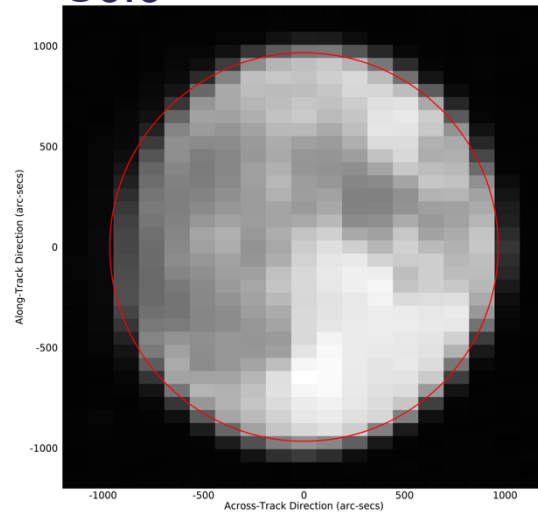
A-Stripe



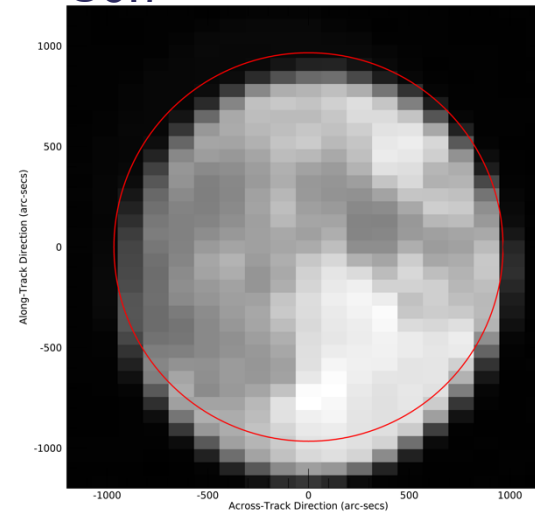
S6.5



S6.6

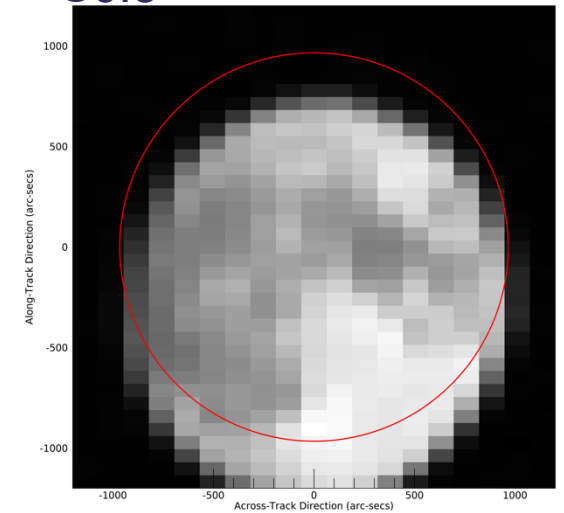


S6.7



S6.8

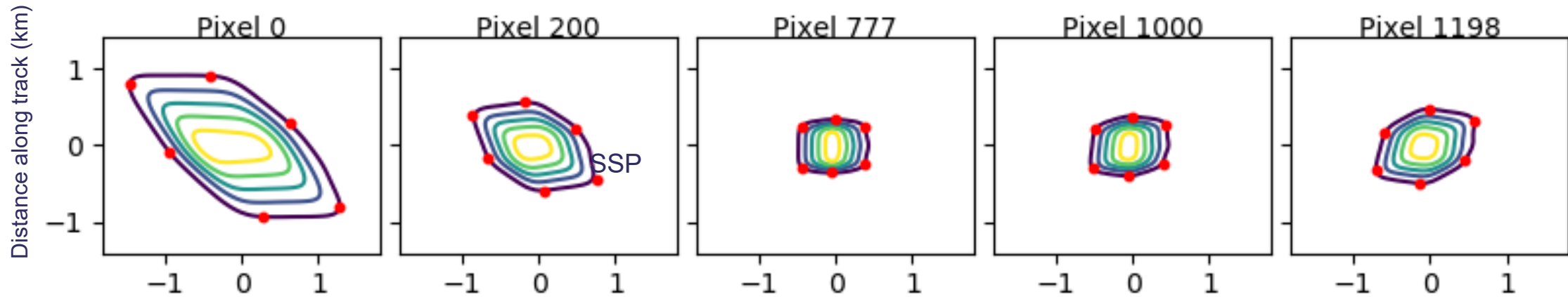
B-Stripe



Field of View + Scan

(Channel S6)

Nadir Pixels - as projected on Earth



Actual field of view in scan direction is defined by IFOV + Integration time (35 us)

The solid angle ($\omega[sr]$) is derived from the ground measurements taking into account the motion of the scanning mirror, the start time and integration time for each channel, and the movement of the satellite along track.

For lunar calibration centre pixel is used – movement is across track only

Deriving Lunar Irradiances from SLSTR

- Standard GSICS approach (See Wu et al). No resampling is performed but the total integrated irradiance is computed using:

$$I_{moon} = \sum L_i \omega_{det} / f_{over}$$

L_i = Radiance measured in pixel i

f_{over} = Oversampling Factor

ω_{det} = Solid angle of detector which is constant so

$$I_{moon} = \omega_{det} \sum L_i / f_{over}$$

- The oversampling factor is determined by

$$f_{over} = FOV_ac_width / ac_interval * FOV_al_width / al_interval$$

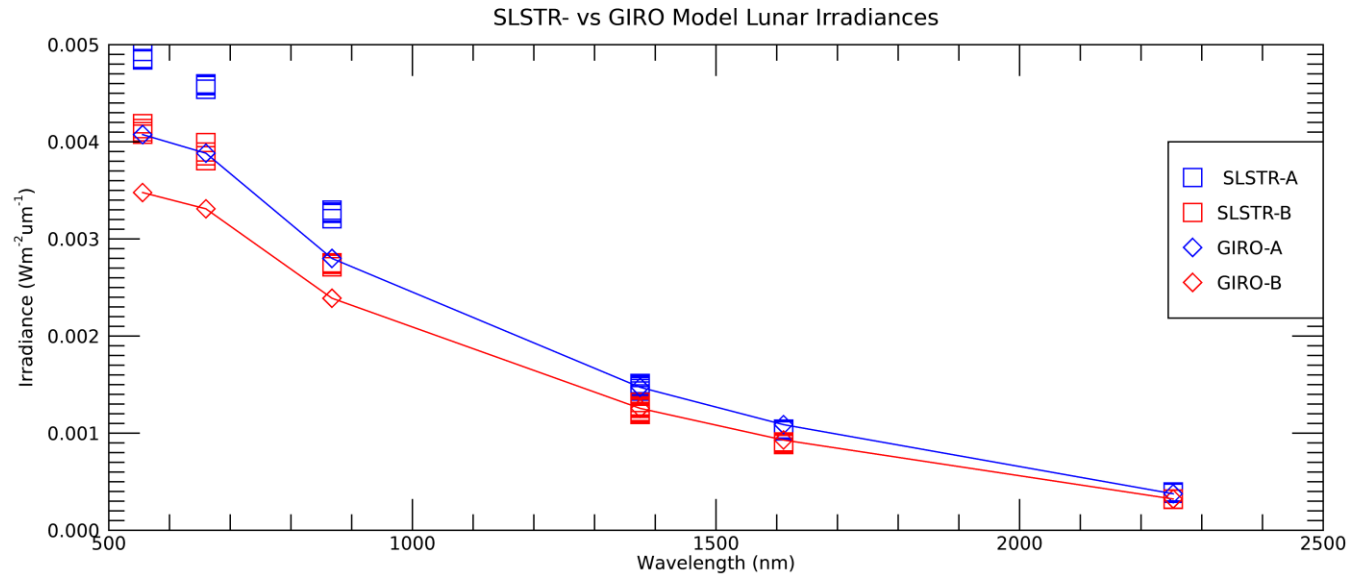
$$= \omega_{det} / (ac_interval * al_interval)$$

So

$$I_{moon} = ac_interval * al_interval \sum L_i$$

So the pixel solid-angle is **NOT** needed to derive irradiance since it cancels. What does matter is the pixel sampling interval.

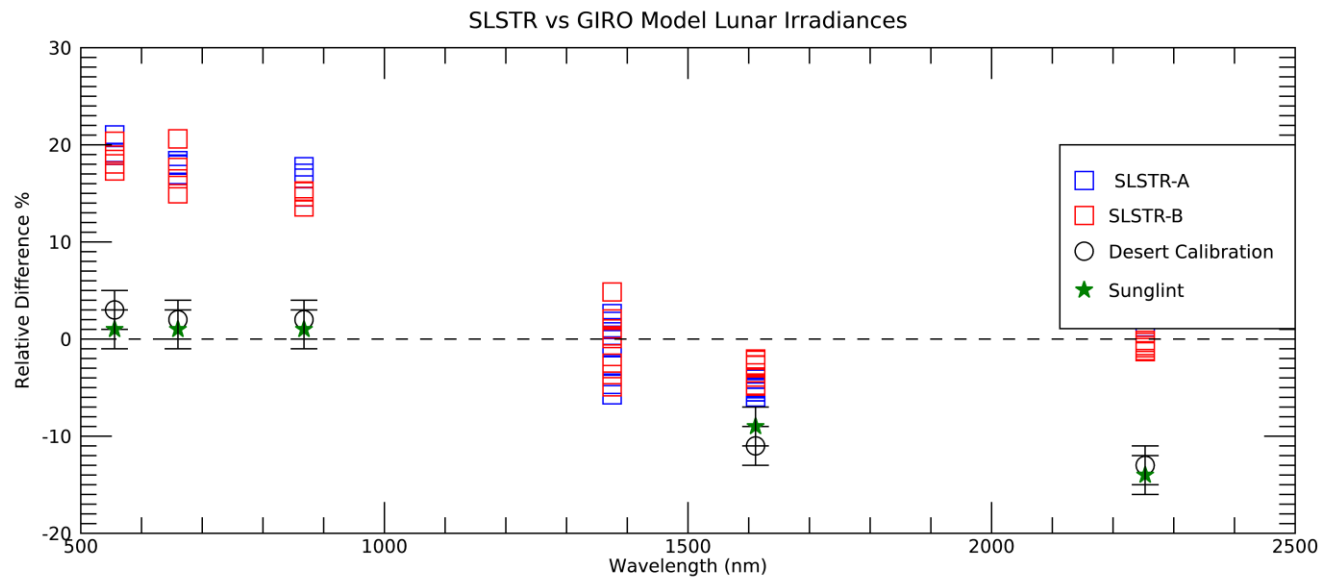
SLSTR vs GIRO



SLSTR-A and B irradiances are consistent with each other.

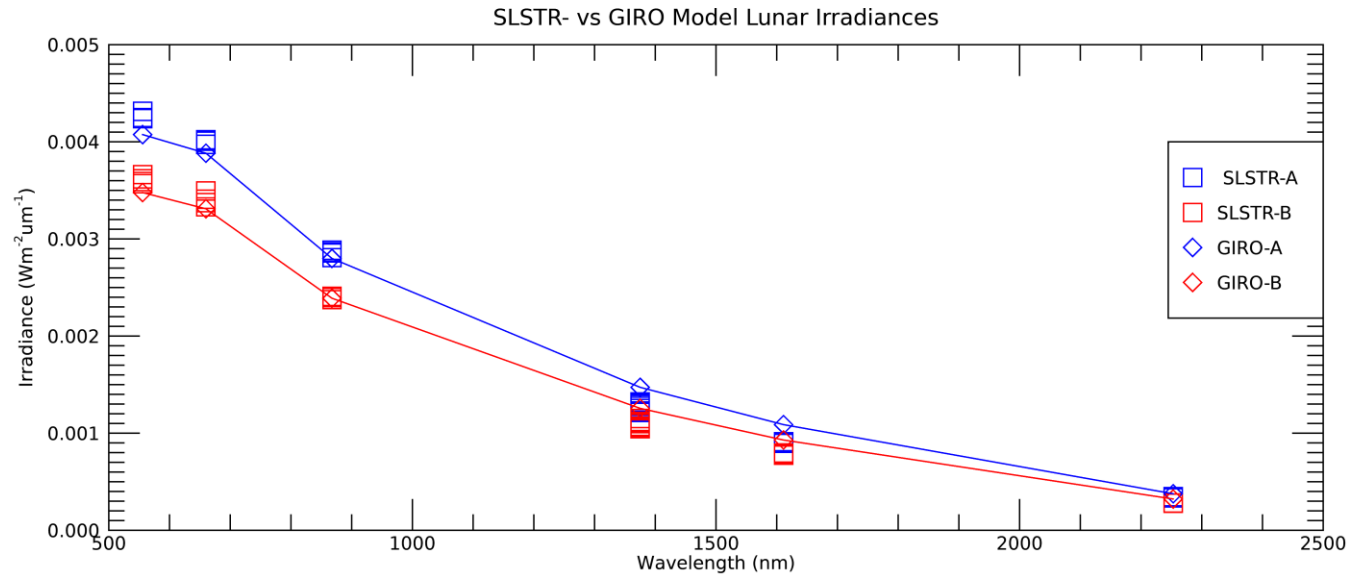
I.e. S3B irradiances $\sim 0.85 \times$ S3A irradiances

Both SLSTR-A and SLSTR-B are \sim high wrt. GIRO data.



Also, comparisons are high wrt. desert calibration and sun-glint results.

SLSTR vs GIRO



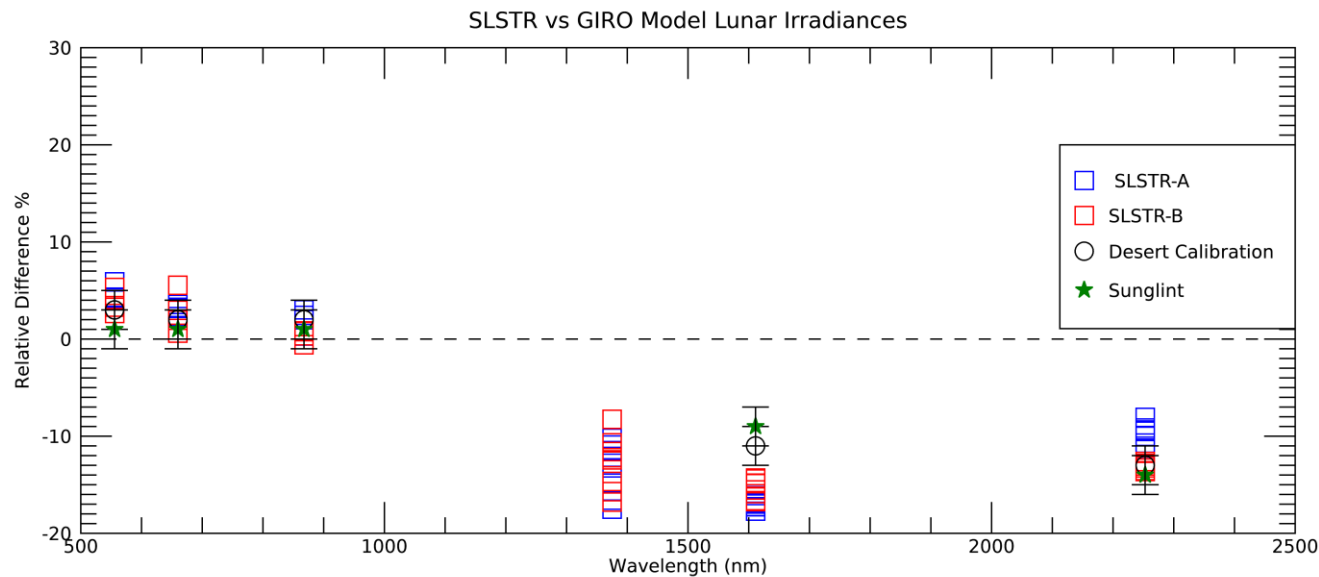
Across-track spacing assumes that detectors are viewing 100% of $40\mu\text{s}$ pixel interval.

However, integration time for SWIR is $35\mu\text{s}$.

If we multiply across-track interval by $35/40$ we now get much better agreement with vicarious calibration.

Is this a happy coincidence?

Note S1-S3 are not integrated but use a filter to match sampling of SWIR channels.



Conclusions

- L0 Monitoring tools have been updated to include dynamic range plots.
- Tool to update S8 and S9 FEE offsets to maintain minimum BT
- Thermal analysis of SLSTR-A and B show temperatures of key optical subsystems have stabilized.
- Uncertainty monitoring has been incorporated into L0 monitoring tools to generate long term trends and per-orbit uncertainty files.
 - MapNoiS3 has been updated to use these files to apply to L1 data products.
- We have developed method for processing SLSTR L0 data containing lunar observations to calibrated irradiances and compared with GIRO reference.